Pergamon

PII: S0306-4522(01)00281-0

www.elsevier.com/locate/neuroscience

Neuroscience Vol. 106, No. 2, pp. 313–330, 2001

0306-4522/01 $20.00+0.00

DOPAMINE REGULATES THE IMPACT OF THE CEREBRAL CORTEX ON THE SUBTHALAMIC NUCLEUS–GLOBUS PALLIDUS NETWORK

P. J. MAGILL, J. P. BOLAM and M. D. BEVAN*

Medical Research Council Anatomical Neuropharmacology Unit, University of Oxford, Mansfield Road, Oxford OX1 3TH, UK

Abstract—The subthalamic nucleus–globus pallidus network plays a central role in basal ganglia function and dysfunction. To determine whether the relationship between activity in this network and the principal afferent of the basal ganglia, the cortex, is altered in a model of Parkinson's disease, we recorded unit activity in the subthalamic nucleus–globus pallidus network together with cortical electroencephalogram in control and 6-hydroxydopamine-lesioned rats under urethane anaesthesia.

Subthalamic nucleus neurones in control and 6-hydroxydopamine-lesioned animals exhibited low-frequency oscillatory activity, which was tightly correlated with cortical slow-wave activity (~1 Hz). The principal effect of dopamine depletion was that subthalamic nucleus neurones discharged more intensely (233% of control) and globus pallidus neurones developed low-frequency oscillatory firing patterns, without changes in mean firing rate. Ipsilateral cortical ablation largely abolished low-frequency oscillatory activity in the subthalamic nucleus and globus pallidus. These data suggest that abnormal low-frequency oscillatory activity in the subthalamic nucleus–globus pallidus network in the dopamine-depleted state is generated by the inappropriate processing of rhythmic cortical input. A component (15–20%) of the network still oscillated following cortical ablation in 6-hydroxydopamine-lesioned animals, implying that intrinsic properties may also pattern activity when dopamine levels are reduced.

The response of the network to global activation was altered by 6-hydroxydopamine lesions. Subthalamic nucleus neurones were excited to a greater extent than in control animals and the majority of globus pallidus neurones were inhibited, in contrast to the excitation elicited in control animals. Inhibitory responses of globus pallidus neurones were abolished by cortical ablation, suggesting that the indirect pathway is augmented abnormally during activation of the dopamine-depleted brain.

Taken together, these results demonstrate that both the rate and pattern of activity of subthalamic nucleus and globus pallidus neurones are altered profoundly by chronic dopamine depletion. Furthermore, the relative contribution of rate and pattern to aberrant information coding is intimately related to the state of activation of the cerebral cortex.

Key words: 6-hydroxydopamine, basal ganglia, electroencephalogram, indirect pathway, oscillation, Parkinson's disease.

The basal ganglia are a collection of subcortical brain nuclei involved in movement, association, cognition and emotion (see reviews by Alexander and Crutcher, 1990; DeLong, 1990; Graybiel, 1995; Gerfen and Wilson, 1996; Schultz et al., 1998). Reciprocally connected glutamatergic neurones of the subthalamic nucleus (STN) and GABAergic neurones of the globus pallidus (GP) form a key network within the basal ganglia (Shink et al., 1996; see review by Smith et al. (1998) and references therein). The principal afferent of the basal ganglia is the cortex, which influences the activity of the STN–GP network directly via monosynaptic projections, or indirectly via GABAergic striatal and glutamatergic thalamic neurones (Kitai and Deniau, 1981; Rouzaire-Dubois and Scarnati, 1985, 1987; Canteras et al., 1990; Ryan and Clark, 1991, 1992; Ryan et al., 1992; Fujimoto and Kita, 1993; Naito and Kita, 1994; Bevan et al., 1995; Mouroux et al., 1995; Maurice et al., 1998; Magill et al., 2000).

Normal information processing within the STN–GP network is characterised by complex spatiotemporal patterns of activity (Georgopoulos et al., 1983; DeLong et al., 1985; Nambu et al., 1990; Aldridge and Gilman, 1991; Anderson and Turner, 1991; Bergman et al., 1994; Wichmann et al., 1994a; Nini et al., 1995). Alterations in the rate and/or pattern of activity in the STN–GP network have been reported in idiopathic and animal models of Parkinson's disease (PD) (Filion, 1979; Filion et al., 1988; Pan and Walters, 1988; Filion and Tremblay, 1991; Hollerman and Grace, 1992; Bergman et al., 1994, 1998; Rothblat and Schneider, 1995; Hassani et al., 1996; Kreiss et al., 1997; Boraud et al., 1998; Magnin et al., 2000; Raz et al., 2000; Vila et al., 2000). Abnormal overactivity of the so-called 'indirect

*Corresponding author. Department of Anatomy and Neurobiology, Health Science Center, College of Medicine, University of Tennessee, 855 Monroe Avenue, Memphis, TN 38163, USA. Tel.: +1-901-448-5965; fax: +1-901-448-7193.

E-mail address: mbevan@utmem.edu (M. D. Bevan).

Abbreviations: ABC, avidin–biotin–peroxidase complex; CV, coefficient of variation of the interspike intervals; DAB, 3,3′-diaminobenzidine tetrahydrochloride; EEG, electroencephalogram; GP, globus pallidus; LFO, low-frequency oscillatory; 6-OHDA, 6-hydroxydopamine; PBS, phosphate-buffered saline; PD, Parkinson's disease; STN, subthalamic nucleus; SWA, slow-wave activity; TH, tyrosine hydroxylase; VTA, ventral tegmental area.

pathway' (striatum-GP–STN-output nuclei) is believed to underlie pathological increases in the firing rate of STN neurones and GABAergic output neurones (Albin et al., 1989; DeLong, 1990). The resultant excessive inhibition of basal ganglia targets has been suggested to underlie symptoms of PD (Albin et al., 1989; DeLong, 1990). It has been proposed more recently that changes in the firing pattern of neurones in the STN–GP network, with or without changes in their overall firing rates, are also of importance (Chesselet and Delfs, 1995; Wichmann and DeLong, 1996; Levy et al., 1997; Bergman et al., 1998; Obeso et al., 2000; Raz et al., 2000). Indeed, STN and GP neurones display more synchronous, bursting patterns of activity, which may be a reflection of emergent, low-frequency oscillatory (LFO) activity within the network (Bergman et al., 1994, 1998; Nini et al., 1995; Raz et al., 2000). Pathological LFO activity in the STN–GP network is associated with resting tremor and may also contribute to other symptoms of PD (Benazzouz et al., 1993; Bergman et al., 1994; Chesselet and Delfs, 1995; Limousin et al., 1995; Nini et al., 1995; Volkmann et al., 1996; Wichmann and DeLong, 1996; Levy et al., 1997; Krack et al., 1998; Rodriguez et al., 1998; Magariños-Ascone et al., 2000; Magnin et al., 2000; Obeso et al., 2000; Raz et al., 2000).

The primary objective of this study was to characterise activity in the STN–GP network in relation to cortical activity in the dopamine-depleted brain. We utilised anaesthetised rats, in which the STN–GP network may be studied in the context of global activity, as determined from the cortical electroencephalogram (EEG). Urethane anaesthesia was used because STN–GP network activity resembles more closely that observed in the unanaesthetised preparation (Pan and Walters, 1988; Magill et al., 2000; Urbain et al., 2000).

We have demonstrated previously that oscillatory activity in the STN–GP network in anaesthetised rats is phase-locked to rhythmic cortical activity and is abolished by transient cortical inactivation (Magill et al., 2000). In contrast, in organotypic co-cultures, oscillatory activity in the STN–GP network persists when cortical input is removed, leading to the proposal that this network acts as a generator of LFO activity in PD (Plenz and Kitai, 1999). Furthermore, neurones in the isolated STN *in vitro* can fire spontaneously in a rhythmic, bursting manner (Beurrier et al., 1999). One explanation for the discrepancy between observations *in vivo* and in culture is that the absence of dopamine in the cultures perturbs the dynamics of the STN–GP network, permitting oscillatory activity to arise independently of the cortex. To test this hypothesis, we recorded single unit activity in the STN–GP network in unilateral 6-hydroxydopamine (6-OHDA)-lesioned (Ungerstedt, 1968) and control animals before and after cortical ablation. Cortical ablation was used in preference to reversible methods of cortical inactivation because (1) using ablation, it is possible to remove consistently the influence of the same area of cortex in different animals; and (2) this consistency can be assessed by histological means.

The symptoms of PD vary according to states of arousal e.g. parkinsonian tremor is associated with quiet wakefulness but disappears during sleep and movement (see review by Elble and Koller, 1990; Rodriguez et al., 1998; Magariños-Ascone et al., 2000). Therefore, oscillatory activity in the STN–GP network may emerge only during certain states of global activity. To test this hypothesis, we compared the activity in the STN–GP network in 6-OHDA-lesioned and control animals during extremes of global activation, in the presence and absence of cortical influence.

EXPERIMENTAL PROCEDURES

Experimental procedures were carried out on adult male Sprague–Dawley rats (Charles River, Margate, UK) and were conducted in accordance with the Animals (Scientific Procedures) Act, 1986 (UK).

Unilateral lesion of dopaminergic neurones and behavioural testing

Unilateral lesions were carried out on 180–220 g rats. Anaesthesia was induced with isoflurane (Isoflo, Schering-Plough Ltd., Welwyn Garden City, UK) and maintained with ketamine (100 mg/kg, i.p.; Ketaset, Willows Francis, Crawley, UK) and xylazine (10 mg/kg, i.p.; Rompun, Bayer, Germany). Twenty five minutes before the injection of 6-OHDA, all animals received a bolus of desipramine (25 mg/kg, i.p.; Sigma, Poole, UK) to minimise the uptake of 6-OHDA by noradrenergic neurones, and pargyline (50 mg/kg, i.p.; Sigma) to maximise the toxic effects on dopaminergic neurones (Schwarting and Huston, 1996a). Animals were then placed in a stereotaxic frame (David Kopf Instruments, Tujunga, CA, USA), a small craniotomy was made directly above the right substantia nigra, and the overlying dura mater was removed. The neurotoxin 6-OHDA (hydrochloride salt; Sigma) was dissolved immediately before use in ice-cold 0.9% w/v NaCl solution containing 0.02% w/v ascorbate to a final concentration of 3 mg/ml. Then 4.5 μl of 6-OHDA solution was injected at a rate of 0.5 μl/min through a steel cannula (0.3 mm outside diameter) attached to a 10-μl Hamilton microsyringe (Cole-Parmer, London, UK) into the region adjacent to the medial substantia nigra (4.5 mm posterior of bregma, 1.2 mm lateral to the midline, and 7.9 mm ventral to the dura). Stereotaxic coordinates were calculated from the atlas of Paxinos and Watson (1986). The cannula was left in place for 5 min before being withdrawn.

Behavioural tests were performed 14 to 15 days after the injection of toxin. The extent of the nigral lesion was assessed by challenge with apomorphine (Hudson et al., 1993; Schwarting and Huston, 1996b). Following a 15 min period in the observation chamber, animals received a single bolus of apomorphine (0.05 mg/kg, s.c.; Sigma) and were returned to the chamber for observation. The number of contraversive and ipsiversive turns were then counted. The lesion was considered successful in those animals that made at least 100 net contraversive rotations in 20 min (Hudson et al., 1993).

Electrophysiological recording and labelling of neurones

Electrophysiological recordings were made in 13 rats (280–510 g), six of which had received successful 6-OHDA lesions. Recordings were made in 6-OHDA-lesioned animals 7 to 25 days after testing with apomorphine. Anaesthesia was induced with isoflurane and maintained with urethane (1.25 g/kg, i.p.; ethyl carbamate, Sigma), and supplemental doses of ketamine and xylazine (30 mg/kg and 3 mg/kg, i.p., respectively). All wound margins were infiltrated with the local anaesthetic, bupivacaine (0.75% w/v; Astra, Kings Langley, UK), and corneal dehydration was prevented with application of Hypromellose eye drops (Norton Pharmaceuticals Ltd., Harlow, UK). Animals were

then placed in a stereotaxic frame. Body temperature was maintained at 37 ± 0.5°C with the use of a homeothermic heating device (Harvard Apparatus Ltd., Edenbridge, UK). Anaesthesia levels were assessed by examination of the EEG, and by testing reflexes to a cutaneous pinch or gentle corneal stimulation. Electrocardiographic activity and respiration rate were also monitored constantly to ensure the animals' well-being. To minimise the effects of contralateral afferent activity in the recorded hemisphere, the corpus callosum was transected in each animal before recording. Following a craniotomy, the corpus callosum was transected under stereotaxic control with a razor blade, set at an angle of 30° to vertical, along the length of the left hemisphere; from 5.0 mm anterior of bregma to 6.5 mm posterior of bregma and along a course that ran 2.0 mm lateral to the midline (see Fig. 1D). Small craniotomies were made directly above the STN or GP and the overlying dura mater was removed. Mineral oil or saline solution (0.9% w/v NaCl) was applied to all areas of exposed cortex to prevent dehydration.

The EEG was recorded via a steel screw juxtaposed to the dura mater above the ipsilateral or contralateral frontal cortex (3.0 mm anterior of bregma and 2.0 or 4.0 mm lateral to the midline, respectively) and referenced against an indifferent electrode placed adjacent to the temporal musculature. Raw EEG was band-pass-filtered (0.1–100 Hz), amplified (2000×) with a NL104 preamplifier (Digitimer Ltd., Welwyn Garden City, UK), collected on tape, and displayed simultaneously on a digital oscilloscope (DSO 610, Gould Instruments, Ilford, Essex, UK).

Extracellular recordings of action potentials of STN or GP neurones were made using 15–25 MΩ glass electrodes (tip diameter ~1.5 μm), which contained saline solution (0.5 M NaCl) and Neurobiotin (1.5% w/v, Vector Labs, Peterborough, UK). Electrode signals were amplified (10×) through the active bridge circuitry of an Axoprobe-1A amplifier (Axon Instruments, Foster City, CA, USA), ac-coupled and amplified a further 100× (ac-dc Amp, Digitimer), before being filtered between 0.4 and 4 kHz (NL125, Digitimer). Signals were collected on tape (60ES DAT system, Sony, UK) and displayed simultaneously on an oscilloscope (Gould Instruments). Spikes were often several mV in amplitude and always exhibited an initial positive deflection. Recordings of spontaneous activity typically lasted for 4–25 min.

Large areas of ipsilateral frontal and parietal cortex were aspirated on the day of electrophysiological recording using suction generated by a polished Pasteur pipette connected to a rubber bulb. The ablative cavity was filled with warm (35–37°C) mineral oil to prevent dehydration. Sensory stimulation was elicited by pinching the contralateral hindpaw with serrated forceps that were driven by a standard pneumatic pressure. Typically, animals did not exhibit a paw withdrawal reflex or a marked change in respiration rate in response to the pinch, although very weak responses were evoked rarely. For multiple recordings, a long interstimulus interval (>15 min) was used to allow recovery of responses.

To identify the location of recorded units, neurones were then labelled with Neurobiotin by the juxtacellular method (Pinault, 1996; Bevan et al., 1998; Magill et al., 2000). In brief, the electrode was advanced slowly towards the neurone while a microiontophoretic current was applied (1–10 nA anodal current, 200 ms duration, 50% duty cycle). The optimal position of the electrode was identified when the firing pattern of the neurone was modulated robustly by current injection. Neuronal firing was modulated by the microiontophoretic current for at least 5 min to obtain reliable labelling. On some occasions when robust modulation could not be achieved, the position of the recorded unit was usually marked by a discrete, extracellular deposit of Neurobiotin (100 nA anodal current; 1 s (50%) duty cycle for 60 min). Animals were then given a lethal dose of anaesthetic and perfused via the ascending aorta with 100 ml of 0.1 M phosphate-buffered saline at pH 7.4 (PBS), followed by 300 ml of 0.1% glutaraldehyde and 4% paraformaldehyde in 0.1 M phosphate buffer, pH 7.4, and then by 150 ml of the same solution without glutaraldehyde. Brains were then post-fixed in the latter solution at 4°C for at least 12 h.

Histochemistry and immunocytochemistry

The extent of the 6-OHDA lesion was assessed by immunocytochemistry for tyrosine hydroxylase (TH). Standard techniques were used to visualise the Neurobiotin-filled cells (Horikawa and Armstrong 1991; Pinault, 1996; Bevan et al., 1998). In brief, the fixed brain was cut into two blocks at the level of the entopeduncular nucleus and sectioned in the coronal plane on a vibrating microtome (rostral blocks including the GP and caudal blocks including the STN and substantia nigra were sectioned at 60 and 40 μm, respectively, to enhance the relative penetration of antibodies in sections containing the nigra). Histochemical and immunocytochemical incubations were carried out at room temperature. Sections were washed in PBS and incubated overnight in mouse anti-TH monoclonal antibody (1:5000 dilution; Sigma) and avidin–biotin–peroxidase complex (ABC; 1:100; Vector) in PBS containing 0.2% Triton X-100 and 1% w/v bovine serum albumin (Sigma). After washing, the sections were incubated in hydrogen peroxide (0.002% w/v; Sigma) and 3,3′-diaminobenzidine tetrahydrochloride (DAB, 0.025% w/v, Sigma) in the presence of nickel ammonium sulphate (0.5% w/v; Sigma) dissolved in Tris buffer (0.05 M, pH 8.0) for 15–30 min. Neurobiotin-filled cells were labelled intensely with an insoluble, black/blue precipitate. Following further washing, the slices were incubated in PBS containing biotinylated-horse anti-mouse IgG antibody (1:200; Vector) for 2 h, washed, and incubated for a further 2 h with ABC (1:100). The slices were then washed and incubated in hydrogen peroxide (0.01% w/v; Sigma) and DAB (0.05% w/v) in Tris buffer (0.05 M, pH 7.4) for 10–20 min. TH-immunoreactive cell bodies, dendritic processes and axons were labelled intensely with an insoluble, brown precipitate. Finally, sections were dehydrated, cleared and mounted for light microscopy using standard techniques (Bolam, 1992).

Data analysis

Unit activity and EEG were sampled at 12 kHz and 200 Hz, respectively, and digitised off-line with the Spike 2 acquisition and analysis software (Cambridge Electronic Design, Cambridge, UK). Data from the recording session were inspected visually and epochs of robust cortical slow-wave activity (SWA) were identified (Magill et al., 2000). In a series of early experiments, visually identified episodes of the strongest SWA were validated for control purposes by spectral analysis (see power spectra below). A portion of the coincident spike train composed of 150 spikes was then isolated and used for statistical analysis. The Lomb algorithm was used to determine the statistical significance and frequency of any periodic discharge features (within the 0.5–50 Hz range) present in the spike train (Kaneoke and Vitek, 1996). Frequency spectra of spiking are displayed as 'Lomb periodograms'. The relative power of a peak in the periodogram is indicated by the clearance of the peak from the significance level of $P = 0.05$ (represented by dashed line in Figs. 2–7). The coefficient of variation of the interspike intervals (CV), a value used widely as an indicator of regularity in point processes (Johnson, 1996), was also calculated. Neurones that did not display significant, low-frequency (≤1.5 Hz) oscillations, as determined using the Lomb algorithm, were further subdivided into regular (CV ≤ 0.35) and irregular (CV > 0.35) firing units. Mean firing frequency was calculated from the reciprocal of the mean interspike interval. As described previously, neurones that discharge in a regular manner often possess a significant frequency of oscillation that is similar to the mean firing rate (Kaneoke and Vitek, 1996; Magill et al., 2000).

Auto-correlograms of action potentials were calculated for the same 150 spikes of data using Mathematica routines (Wolfram Research Inc., Long Hanborough, UK) based on standard methods and a bin size of 10 ms (Perkel et al., 1967; Abeles, 1982). Spike-triggered waveform averaging of the coincident EEG was performed with Spike 2 and was used to estimate phase relationships. Power spectra of the coincident EEG were calculated using the Fast Fourier Transform function of Spike

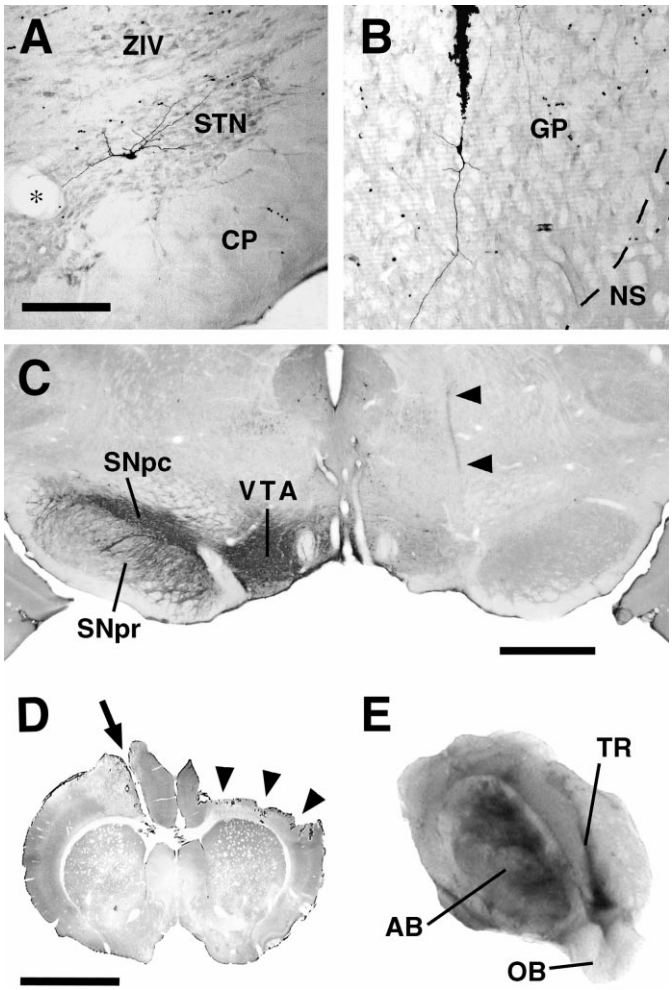

Fig. 1. Anatomical verification of recording sites, unilateral nigral lesions and surgical manipulations. (A, B) Light micrographs of STN and GP neurones that were labelled juxtacellularly with Neurobiotin. (A) The STN neurone was located near the centre of the nucleus. The STN lies dorsal to the cerebral peduncle (CP) and is characterised by a higher density of neurones compared to the overlying ventral division of the zona incerta (ZIV). A large blood vessel (*) lies on the border between medial STN and ZIV. (B) The GP neurone was situated near the centre of the rostral half of the GP. Note the track of the electrode above the labelled neurone. The border (dashed line) between the GP and the neostriatum (NS) is also indicated. Scale bar in (A) also applies to (B) = 200 μm. (C) Light micrograph of a coronal section though the midbrain of a 6-OHDA-lesioned rat, which was stained to reveal TH. Intense TH immunoreactivity was observed in the left substantia nigra pars compacta (SNpc) and VTA and lighter labelling was observed in the substantia nigra pars reticulata (SNpr). Staining for TH was virtually absent in the right hemisphere. Note also the trajectory of the injection cannula (between arrowheads). Scale bar = 1 mm. (D) Photomicrograph of a coronal section from a transected and ablated control rat, at the level of the neostriatum. The majority of the right frontal and parietal cortices were ablated (arrowheads) and the corpus callosum was transected close to the midline in the left hemisphere (arrow). Scale bar = 4 mm. (E) Digital image of a brain from a transected and ablated rat. The callosal transection (TR) extended along the length of the left hemisphere. The ablative cavity (AB) encompassed the frontal and parietal cortical areas of the right hemisphere. OB, olfactory bulbs.

2. Statistical comparisons of firing rates and oscillation frequencies were conducted using the Mann–Whitney *U*-test. The Wilcoxon signed rank test was used to compare paired data (e.g. pinch effects). The significance level for all tests was taken to be $P < 0.05$. Data are expressed as mean ± S.D.

RESULTS

Location of recorded neurones

After physiological characterisation, juxtacellular microiontophoresis led in each case to a single neurone being well labelled (Fig. 1A, B): 46 of 181 recorded neurones were labelled using this technique. The locations of the remainder were determined directly from extracellular deposits of Neurobiotin or inferred from the stereotaxic position of the recorded unit relative to deposits or juxtacellularly labelled neurones. All regions of the STN and the rostral half of the GP were sampled in control and 6-OHDA-lesioned animals.

Extent of 6-OHDA lesions

A successful nigral lesion, as inferred from behavioural testing, was confirmed in each animal by a near complete loss of TH-immunoreactive neurones from the substantia

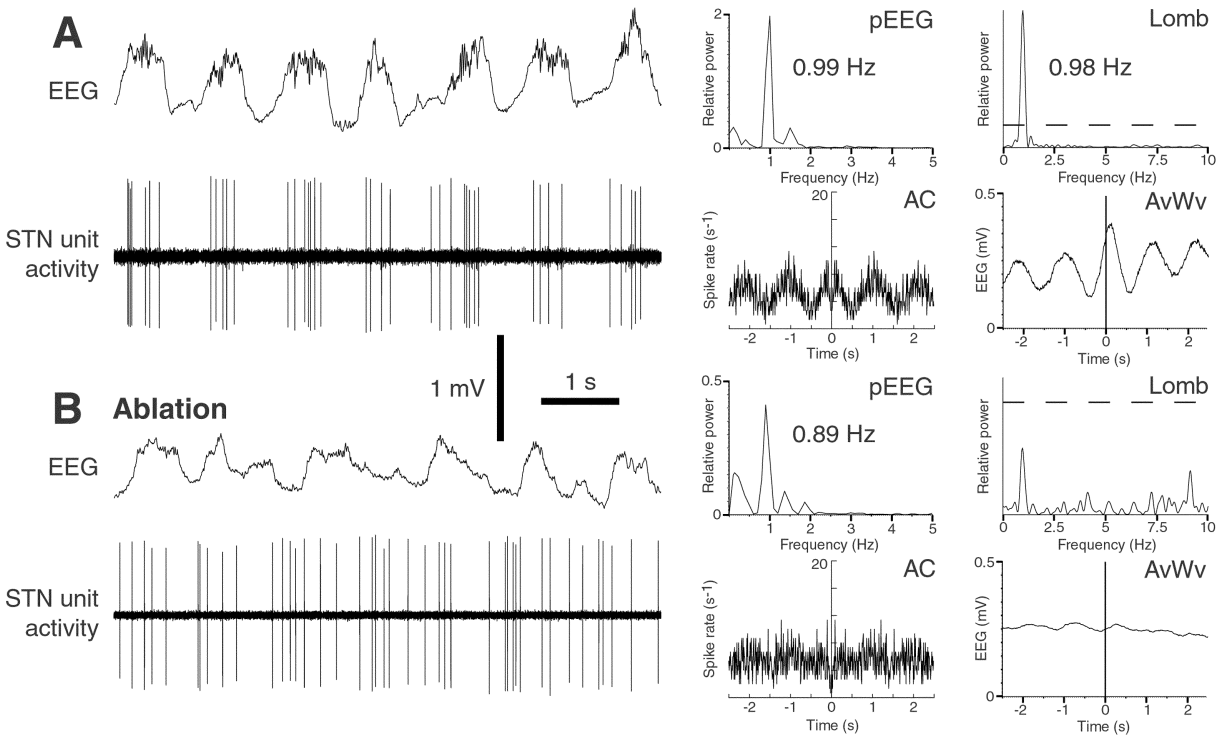

Fig. 2. Neuronal activity in the STN of control rats is related closely to coincident cortical activity. (A) LFO STN neurone (CV = 0.99; mean rate = 6.0 Hz). The neurone fired predominantly during the active component of the cortical slow-wave; the active component was seen in the EEG trace as periods of superimposition of small-amplitude, high-frequency events on the peaks of the large-amplitude slow-wave. Rhythmic spike firing was apparent from the broad peaks in the auto-correlogram (AC). Comparison of the Lomb periodogram (Lomb) with the power spectrum of the EEG (pEEG) indicated a similar frequency of rhythmic activity in the STN spike train and cortex. The dashed line in this and subsequent Lomb periodograms denotes a significance level of $P = 0.05$. The phase relationship between spiking and the EEG is shown on the spike-triggered waveform average (AvWv). (B) Irregular firing STN neurone (CV = 0.65; mean rate = 5.9 Hz) recorded after ipsilateral cortical ablation. The discharge was not correlated with contralateral cortical EEG and did not display a significant oscillatory component. Note that the CV values of each neurone reflected the differences in firing pattern observed. Neurones were recorded in the same animal. Calibration bars apply to both left hand panels. In this and subsequent figures, AC designates auto-correlograms of spiking activity (bin size 10 ms), Lomb designates Lomb periodograms of spiking activity, pEEG designates power spectra of the coincident EEG, and AvWv designates spike-triggered averages of the EEG waveform.

nigra of the right hemisphere (Fig. 1C). The ventral tegmental area (VTA) was also affected in all animals, but to differing extents.

Verification of callosal transections and cortical ablations

In each animal, the corpus callosum was transected near the midline and along the rostral-caudal extent of the forebrain of the left hemisphere (Fig. 1D, E). Thus, transection largely isolated the recorded hemisphere from the contralateral cortex. Large areas of the right prefrontal, frontal and parietal cortices were also acutely ablated in each animal (Fig. 1D, E). Ablation of neighbouring medial cortical areas (infralimbic, prelimbic, cingulate, retrosplenial) was not attempted due to the proximity of the superior sagittal sinus. Ventral and lateral cortical regions (orbital, agranular, insular, piriform, parietal area 2) were also left intact. Thus, cortical ablation removed a large proportion of the cortical afferents to the basal ganglia of the right hemisphere.

EEG activity

Prevailing cortical activity was assessed from EEG recordings. As described previously (Steriade et al., 1993c; Magill et al., 2000), surgical anaesthesia was accompanied by regularly occurring slow-waves of large amplitude (>400 μV) in the frontal EEG (Figs. 2–7). Higher-frequency activity, which was of smaller amplitude (<200 μV), was often superimposed on specific portions of the slow-wave (e.g. Fig. 2A). These parts of the slow-wave are associated with synchronous spike discharges in cortical projection neurones and will be referred to as the 'active component' (Amzica and Steriade, 1995; Steriade et al., 1996; Steriade and Amzica, 1998). The frequency range of the smaller amplitude waves varied widely but spindle activity in the range of 7–14 Hz was observed often (Steriade et al., 1993d; McCormick and Bal, 1997; Amzica and Steriade, 1998; Steriade and Amzica, 1998).

Firing properties of STN neurones in control and 6-OHDA-lesioned animals before and after cortical ablation

The relationship between activity in the cortex and the STN–GP network was examined by simultaneous recording of units and the EEG. Consistent with pre-

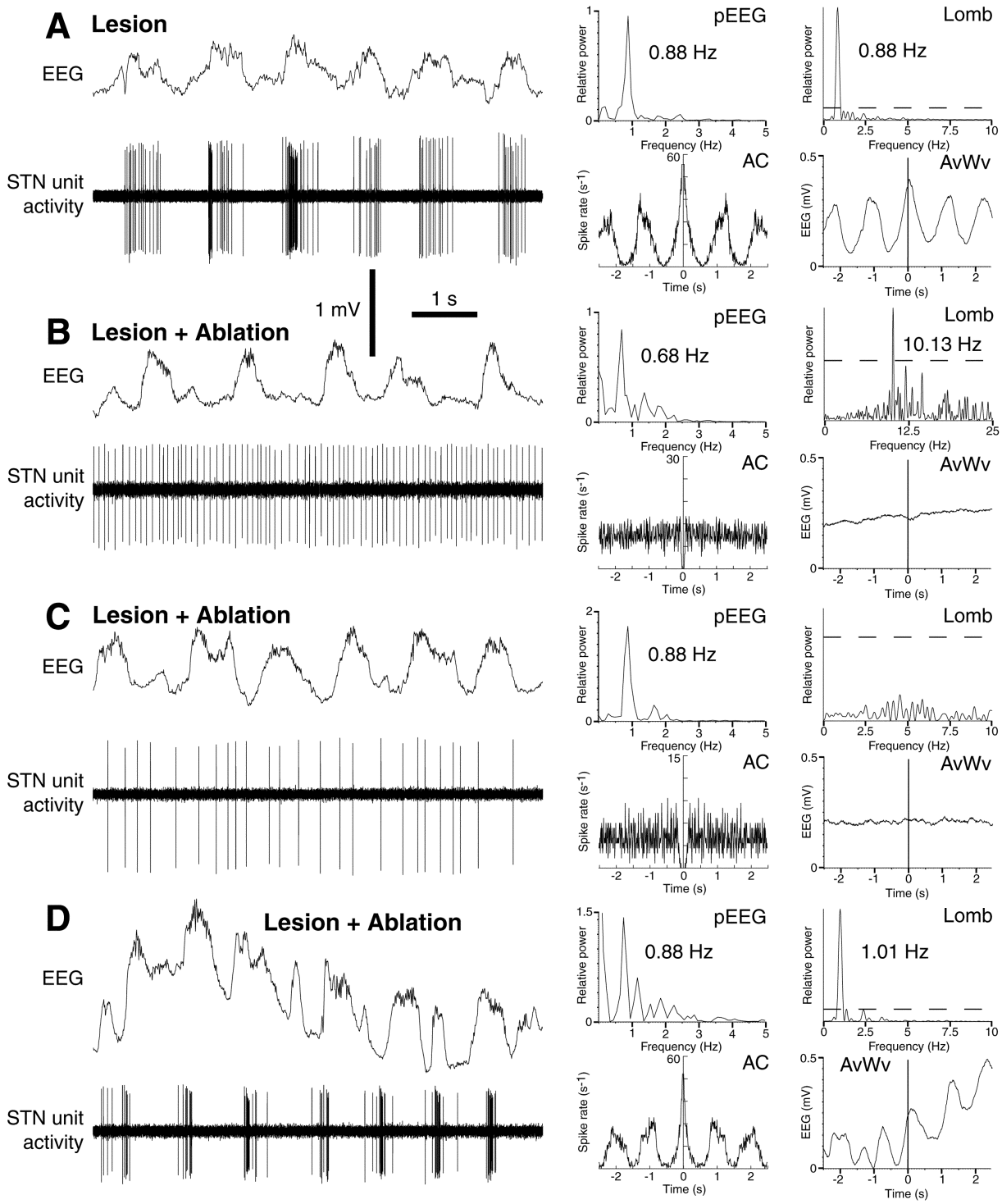

Fig. 3. Neuronal activity in the STN of 6-OHDA-lesioned rats is related closely to coincident cortical activity. (A) LFO STN neurone (CV = 2.35; mean rate = 15.8 Hz) recorded in a 6-OHDA-lesioned animal. The neurone discharged powerfully during the active component of the cortical slow-wave. Comparison of the Lomb periodogram with the power spectrum showed identical frequencies of rhythmic activity in the spike train and EEG. In 6-OHDA-lesioned animals, the mean rate of firing of STN neurones was higher than that in control animals. (B) Cortical ablation in 6-OHDA-lesioned animals abolished LFO activity and reduced the mean rates of firing in the majority of STN neurones. Regular firing STN neurone (CV = 0.32; mean rate = 9.9 Hz) recorded after cortical ablation. Activity was not related to coincident SWA. The neurone exhibited a mean firing rate that was similar to the dominant frequency of activity in the Lomb periodogram. (C) Irregular firing STN neurone (CV = 0.44; mean rate = 4.1 Hz) recorded after cortical ablation. (D) LFO neurone (CV = 2.12; mean rate = 12.5 Hz) recorded after cortical ablation. Twenty percent of STN neurones continued to oscillate at a low frequency after ablation and discharge was correlated weakly with SWA in the contralateral cortex. Note that the CV values of each neurone reflected the differences in firing pattern observed. Neurones in (A–C) were recorded in the same animal. Calibration bars apply to all left hand panels.

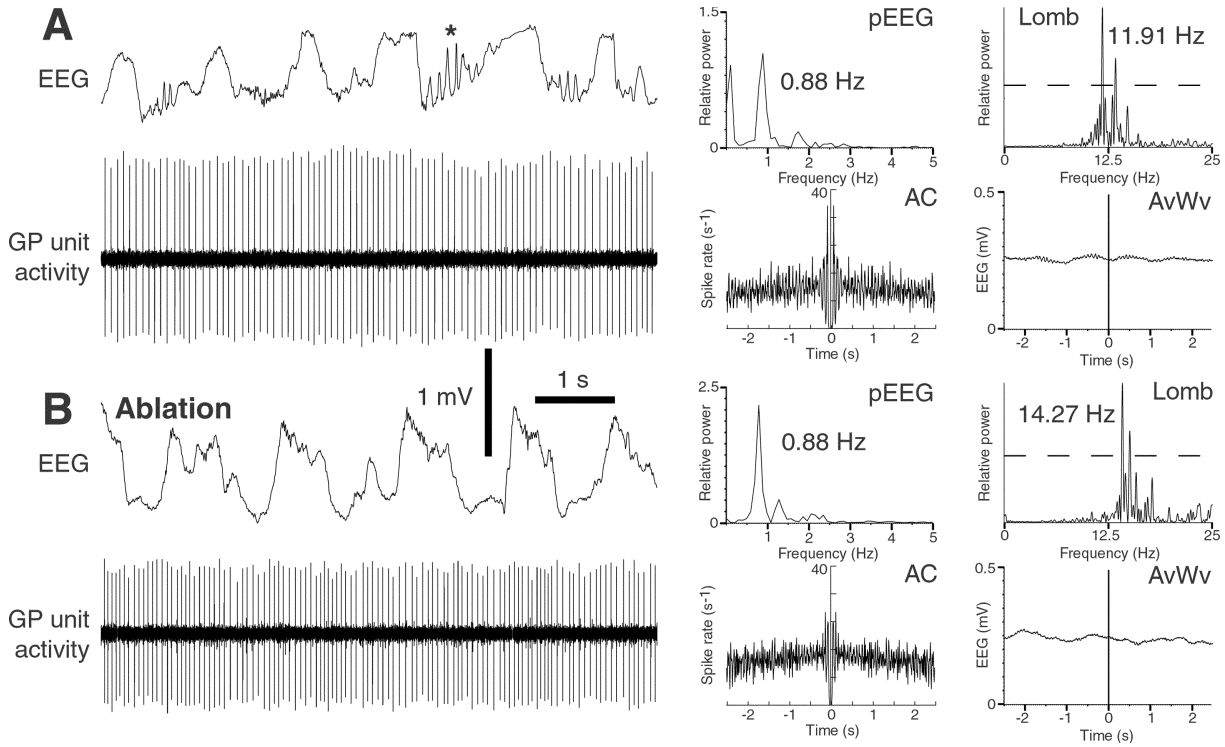

Fig. 4. Neuronal activity in the GP of control rats is not related closely to coincident cortical activity. (A) Regular firing GP neurone (CV = 0.15; mean rate = 12.5 Hz). The GP neurone displayed a highly regular, single-spike firing pattern that was maintained during episodes of robust SWA. Thus, the pEEG and Lomb periodogram were dissimilar, broad peaks were not observed in the AC, and the AvWvs were almost flat. The occurrence of spindle sequences (*) in the EEG had no detectable effect on firing rate or pattern. (B) Regular firing GP neurone (CV = 0.22; mean rate = 14.9 Hz) recorded in the same animal after cortical ablation. The rate and pattern of firing of GP neurones was not altered by ablation. Calibration bars apply to both left hand panels.

vious observations (Magill et al., 2000), extracellular unit recordings revealed that STN neurones exhibited LFO firing patterns during periods of robust SWA in the ipsilateral cortex of control animals (Fig. 2A, Table 1). When the active component of the slow-wave was observed clearly, the discharge of STN neurones was restricted predominantly to this component. Spectral and correlation analyses revealed that the frequency at which these envelopes of spiking activity occurred matched closely the predominant frequency of the coincident cortical slow-wave (Fig. 2A, Table 1). Following ipsilateral cortical ablation, LFO firing in STN neurones was abolished (Fig. 2B, Table 1). During periods of robust SWA in the contralateral cortex, STN neurones discharged in an irregular or regular manner throughout the entire cycle of the cortical slow-wave and the activity of STN neurones no longer matched the frequency of the coincident slow oscillation (Fig. 2B, Table 1). These data confirm that the pattern and frequency of firing of STN neurones in control animals is correlated tightly with coincident activity in the ipsilateral cortex.

To determine whether the depletion of dopamine alters the impact of the cortex on the STN–GP network and whether it perturbs the dynamics of the STN–GP network, permitting oscillatory activity to arise independently of the cortex, we recorded EEG and coincident unit activity in 6-OHDA-lesioned rats before and after cortical ablation. As in control animals, unit recordings in 6-OHDA-lesioned animals revealed that STN neurones displayed LFO firing patterns during periods of robust SWA in the ipsilateral cortex (Fig. 3A, Table 1). Subthalamic nucleus neurones again discharged predominantly during the active component of the slow-wave. The frequencies at which these epochs of activity occurred matched closely the frequencies of the coincident slow-wave and were not significantly different from control animals (Fig. 3A, Table 1). However, the mean rate of firing was significantly higher in 6-OHDA-lesioned animals compared to control animals (233.3% of control; $P < 0.001$). As in control animals, following cortical ablation LFO firing was not recorded in the majority (80%) of STN neurones (Fig. 3B–D, Table 1). Thus, even during periods of robust SWA in the contralateral cortex, most STN neurones discharged in a regular or irregular manner during both the inactive and active components of the slow-wave (Fig. 3B–D, Table 1). Those neurones firing in a regular manner displayed a significant peak in their Lomb periodogram at a frequency that matched closely the mean rate of firing (Fig. 3B, Table 1). The mean discharge rate of STN neurones following ablation was significantly lower than before ablation (30.1% of firing rate before ablation; $P < 0.0001$). These observations demonstrate that the impact of the cortex on activity in the STN is greater following the depletion of dopamine, and that oscillatory activity in the STN is largely directed by the cortex in this preparation.

In contrast to control animals, about 20% of STN

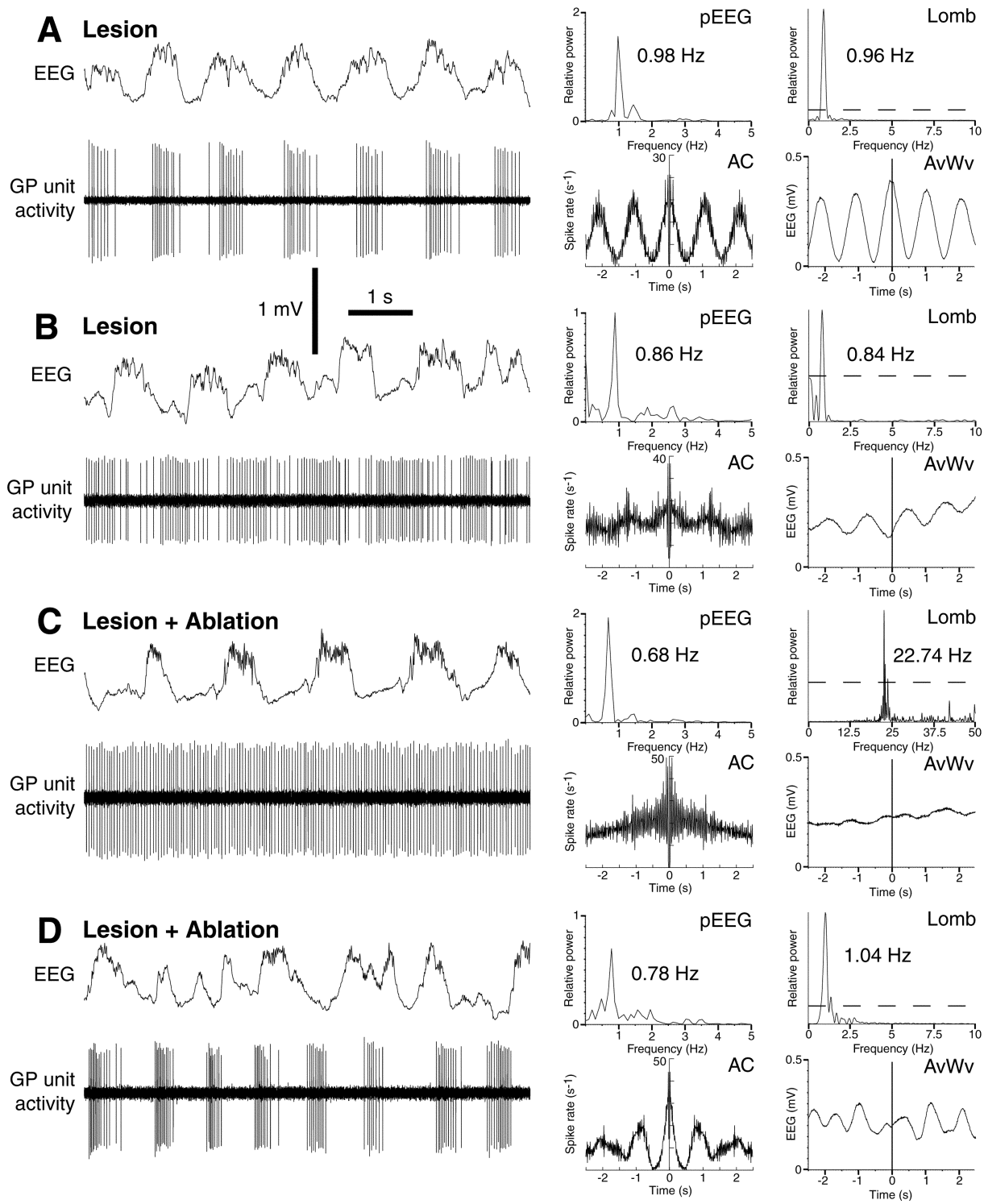

Fig. 5. Neuronal activity in the GP of 6-OHDA-lesioned rats is correlated tightly with coincident cortical activity. (A) LFO GP neurone (CV = 1.48; mean rate = 9.5 Hz) that fired predominantly during the active component of the cortical slow-wave. Rhythmic spike firing was manifest clearly as broad peaks in the AC. (B) LFO GP neurone (CV = 0.75; mean rate = 19.0 Hz) that discharged predominantly during the trough (inactive component) of the cortical slow-wave. The dramatic alteration in firing pattern that was observed in 6-OHDA-lesioned animals (cf. GP neurone in Fig. 4A) was not associated with a change in mean firing rate. (C) Regular firing GP neurone (CV = 0.19; mean rate = 23.1 Hz) recorded after ipsilateral cortical ablation. Most of the GP neurones recorded after ablation fired in a tonic, regular manner that was not statistically different from the regular firing patterns observed in control animals and was not related to coincident contralateral EEG. (D) LFO GP neurone (CV = 2.03; mean rate = 12.4 Hz) recorded after cortical ablation. This form of activity was observed in 15% of GP neurones after ablation. The activity of this neurone was correlated weakly with contralateral cortical SWA. Neurones in (A, C, D) were recorded in the same animal. Calibration bars apply to all left hand panels.

Table 1. Firing properties of STN neurones

	Control		6-OHDA-lesioned	
	Intact cortex	Ablated cortex	Intact cortex	Ablated cortex
Number of observations	28	10	33	15
LFO neurones[a]	28	0	33	3
Irregular neurones	0	8	0	7
Regular neurones	0	2	0	5
Firing rate (Hz)				
All neurones	8.1 ± 2.9	5.7 ± 4.3	18.9 ± 12.2	5.8 ± 4.2
LFO neurones	8.1 ± 2.9	–	18.9 ± 12.2	7.2 ± 4.8
Irregular neurones	–	5.1 ± 4.5	–	2.7 ± 1.7
Regular neurones	–	7.9 ± 4.0	–	9.4 ± 3.4
Coefficient of variation				
LFO neurones	1.30 ± 0.36	–	2.27 ± 0.82	1.75 ± 0.39
Irregular neurones	–	0.66 ± 0.25	–	0.91 ± 0.47
Regular neurones	–	0.26 ± 0.01	–	0.30 ± 0.08
Number of oscillating neurones	28	2	33	8
LFO neurones	28	0	33	3
Irregular neurones	0	0	0	0
Regular neurones	0	2	0	5
Frequency of spike train oscillation (Hz)				
LFO neurones	0.84 ± 0.10	–	0.88 ± 0.20	0.89 ± 0.14
Irregular neurones	–	–	–	–
Regular neurones	–	8.06 ± 4.57	–	9.41 ± 3.24
Frequency of cortical SWA (Hz)[b]	0.83 ± 0.09	0.84 ± 0.09	0.88 ± 0.18	0.91 ± 0.21

[a]Neurones were defined as displaying a significant, low-frequency oscillation in their spike trains (frequency of ≤ 1.5 Hz; $P < 0.05$).
[b]Cortical SWA was determined from contralateral frontal EEG in the case of neurones recorded after ablation of ipsilateral cortex. Data are expressed as mean ± S.D.

neurones recorded in 6-OHDA-lesioned animals displayed LFO firing even after ablation of the ipsilateral cortex. The frequency of neuronal oscillation was similar to coincident SWA in the contralateral cortex and the spike-triggered waveform average displayed peaks, which suggested that there was a correlation in activity (Fig. 3D).

Firing properties of GP neurones in control and 6-OHDA-lesioned animals before and after cortical ablation

In agreement with previous observations (Magill et al., 2000), all GP neurones recorded in control animals exhibited a tonic, regular firing pattern during robust SWA (Fig. 4A). Quantitative analyses confirmed the regular nature of firing as the mean peak frequency in Lomb periodograms was not significantly different from mean firing rates (Table 2). Neuronal firing rate and pattern were relatively insensitive to minor fluctuations in SWA (Fig. 4A). The discharge of GP neurones was not significantly altered by cortical ablation (Fig. 4B), suggesting that the firing pattern and frequency of GP neurones in control animals under urethane anaesthesia is not influenced strongly by coincident, rhythmic cortical activity.

To further examine the effects of a reduction of dopamine levels on the STN–GP network and its relationship with the cortex, we recorded EEG and coincident unit activity in the GP in 6-OHDA-lesioned rats. In contrast to control animals, the majority of GP neurones recorded in the 6-OHDA-lesioned rats exhibited LFO firing patterns during robust cortical SWA (Fig. 5A, B, Table 2). During periods of robust SWA in the ipsilateral cortex, when the active component of the slow-wave was most clearly seen, oscillatory GP neurones discharged predominantly during the active or inactive components of the slow-wave (Fig. 5A, B, respectively). Neurones discharging predominantly during the active or inactive components were distributed similarly throughout the GP (data not shown). The majority (89%) of neurones displayed a significant peak oscillation in their Lomb periodogram that was similar to the frequency of the coincident slow-wave (Fig. 5A, B, Table 2). Unlike neurones of the STN, the mean firing rates of GP neurones in 6-OHDA-lesioned and control animals were not significantly different.

Following cortical ablation, 85% of GP neurones recorded in 6-OHDA-lesioned animals did not display significant low-frequency oscillations and thus, firing was not correlated with the contralateral cortical oscillation (Fig. 5C, Table 2). Furthermore, the firing rates of regularly discharging GP neurones in 6-OHDA-lesioned animals after ablation were not significantly different from those recorded in control animals before or after cortical ablation. These results indicate that following dopamine depletion, rhythmic cortical activity is propagated to the GP and underlies the emergence of rhythmic bouts of high-frequency firing in the majority of GP neurones. However, about 15% of GP neurones recorded in 6-OHDA-lesioned animals still displayed LFO firing after ablation of the cortex. The frequency of neuronal oscillation was similar to coincident SWA in the contralateral cortex and the spike-triggered waveform average displayed peaks, which suggested that there was a correlation in activity (Fig. 5D).

Response of STN and GP neurones to global activation in control and 6-OHDA-lesioned animals before and after cortical ablation

To characterise the effects of global activation on the STN–GP network in the control and dopamine-depleted conditions, we recorded the responses of the EEG and coincident unit activity to sensory stimulation by hind-paw pinch. This sensory stimulation obliterated the SWA in the cortex, a process hereafter referred to as 'activation', and was always associated with changes in the rate and pattern of firing of STN and GP neurones in control and 6-OHDA-lesioned animals (Figs. 6 and 7).

The ipsilateral cortical activation that followed hind-

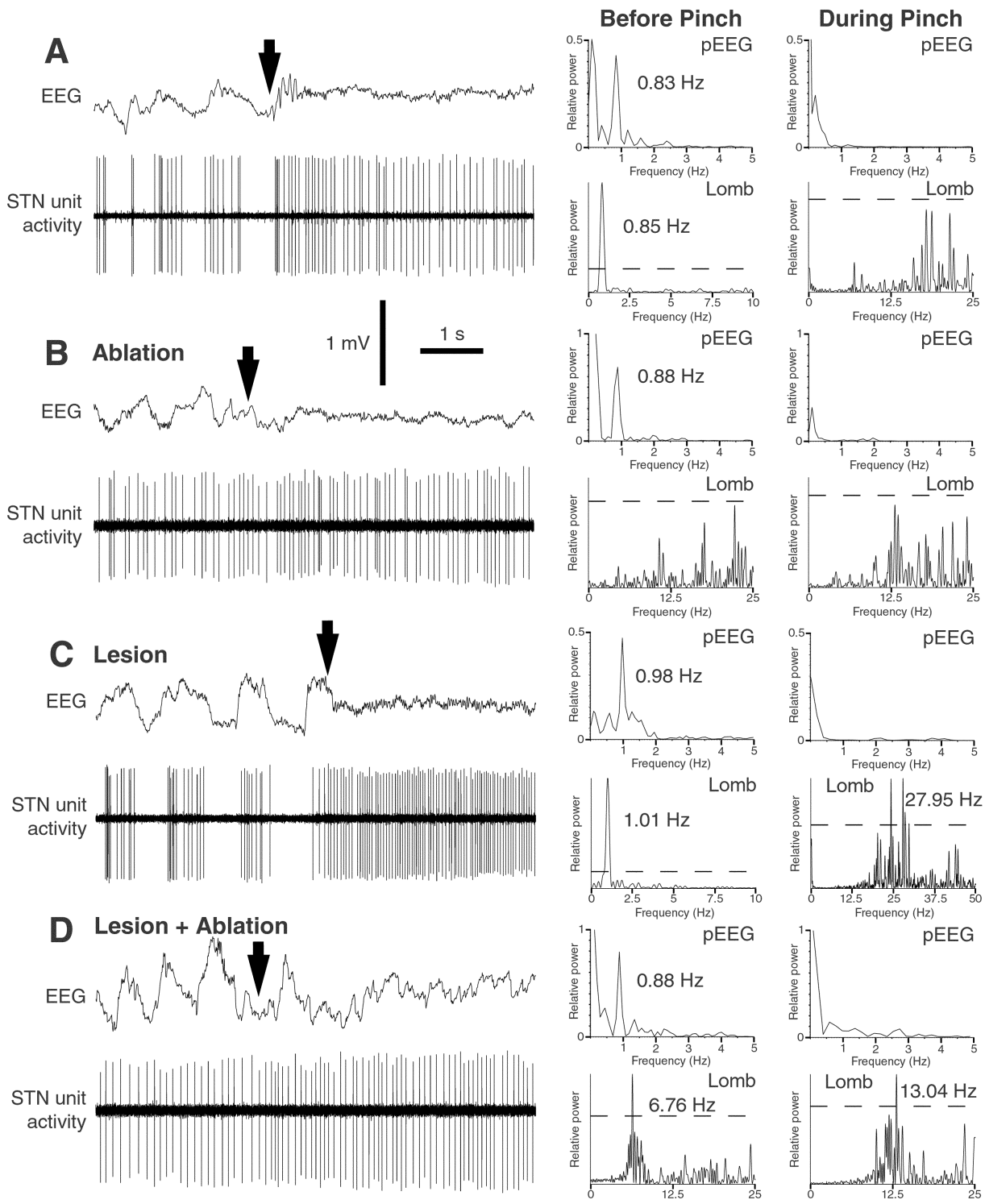

Fig. 6.

Table 2. Firing properties of GP neurones

	Control		6-OHDA-lesioned	
	Intact cortex	Ablated cortex	Intact cortex	Ablated cortex
Number of observations	18	29	28	20
LFO neurones[a]	0	0	25	3
Irregular neurones	0	0	3	1
Regular neurones	18	29	0	16
Firing rate (Hz)				
All neurones	18.0 ± 6.3	17.0 ± 8.3	21.7 ± 8.6	18.7 ± 7.3
LFO neurones	–	–	22.2 ± 8.5	14.6 ± 2.8
Irregular neurones	–	–	17.3 ± 9.0	5.3
Regular neurones	18.0 ± 6.3	17.0 ± 8.3	–	20.31 ± 7.0
Coefficient of variation				
LFO neurones	–	–	1.11 ± 0.39	1.53 ± 0.44
Irregular neurones	–	–	0.67 ± 0.18	0.45
Regular neurones	0.23 ± 0.05	0.17 ± 0.04	–	0.16 ± 0.04
Number of oscillating neurones	18	29	25	19
LFO neurones	0	0	25	3
Irregular neurones	0	0	0	0
Regular neurones	18	29	0	16
Frequency of spike train oscillation (Hz)				
LFO neurones	–	–	0.92 ± 0.22	0.88 ± 0.16
Irregular neurones	–	–	–	–
Regular neurones	18.63 ± 5.96	17.07 ± 8.41	–	19.87 ± 6.96
Frequency of cortical SWA (Hz)[b]	0.89 ± 0.10	0.89 ± 0.21	0.92 ± 0.21	0.92 ± 0.19

[a]Neurones were defined as displaying a significant, low-frequency oscillation in their spike trains (frequency of ≤ 1.5 Hz; $P < 0.05$).
[b]Cortical SWA was determined from contralateral frontal EEG in the case of neurones recorded after ablation of ipsilateral cortex. Data are expressed as mean ± S.D.

paw pinch abolished significant LFO activity in the spike trains of STN neurones recorded in control and 6-OHDA-lesioned animals. All STN neurones adopted a tonic, regular or irregular firing pattern with an increased mean rate of activity (Fig. 6A, C, Table 3; neurones in control animals increased firing to 145.5 ± 32.0% of spontaneous firing rates, $n = 17$, $P < 0.001$; neurones in 6-OHDA-lesioned animals increased firing to 228.6 ± 100.0%, $n = 16$, $P = 0.002$). The mean increase in STN activity was significantly greater in 6-OHDA-lesioned animals than in control animals ($P = 0.023$). LFO activity in the STN only resumed when SWA reappeared in the EEG (data not shown).

After ablation of the ipsilateral cortex, global activation, as monitored by activity in the contralateral cortex, was also accompanied by changes in the rate and pattern of firing of STN neurones (Fig. 6B, D). During activation, STN neurones recorded in control and dopamine-depleted animals displayed a tonic, regular or irregular firing pattern with an increased mean rate (Fig. 6B, D; firing rates increased to 131.7 ± 28.7% of spontaneous firing rates in control animals, $n = 7$, $P = 0.018$; increased to 150.6 ± 62.0% in 6-OHDA-lesioned animals, $n = 9$, $P = 0.011$). Alterations in firing pattern during global activation were minor and were evident as small changes in CVs (Fig. 6B, D).

In the GP of control animals, global activation was associated with tonic, regular or irregular firing patterns and an increased mean rate of activity (Fig. 7A, Table 3; 142.0 ± 19.1% of spontaneous firing rates, $n = 16$, $P < 0.001$). During cortical activation in 6-OHDA-lesioned animals, GP neurones displayed tonic, regular or irregular firing patterns and significant LFO activity was abolished (Fig. 7C, D). Furthermore, in marked contrast to the responses of GP neurones in control animals, a large proportion of GP neurones (61%) in

Fig. 6. Cortical activation alters the firing pattern and increases the firing rate of STN neurones in control and 6-OHDA-lesioned rats. (A) LFO STN neurone recorded in a control animal before and during sensory stimulation by hindpaw pinch. The pinch obliterated cortical SWA (7 s duration; starts at arrow), which resulted in a loss of LFO activity and increased the mean firing rate of the STN neurone (CV = 1.07 mean = 7.0 Hz, before pinch; CV = 0.45, mean = 10.5 Hz, during pinch). The pEEGs and Lomb periodograms in the middle and right hand panels in this and the following figure were determined before and during the pinch, respectively. LFO unit activity swiftly resumed when robust SWA was restored in the EEG (data not shown). (B) Irregular firing STN neurone recorded in a control animal after cortical ablation (CV = 0.50; mean = 9.4 Hz, before pinch). Sensory stimulation (arrow) abolished contralateral SWA and led to an increase in firing frequency (CV = 0.42; mean = 11.9 Hz, during pinch). (C) LFO STN neurone recorded in a 6-OHDA-lesioned animal (CV = 1.54; mean = 9.1 Hz, before pinch). Obliteration of cortical SWA by hindpaw pinch (arrow) altered STN unit activity; LFO activity was lost and there was a dramatic increase in the mean firing rate (CV = 0.28; mean = 22.7 Hz, during pinch). LFO unit activity resumed when robust SWA recovered (data not shown). (D) Regular firing STN neurone (CV = 0.23; mean = 7.0 Hz, before pinch) recorded in a 6-OHDA-lesioned animal after cortical ablation. Activation of contralateral cortex (arrow) was associated with a modest increase in the mean firing rate of the STN neurone (CV = 0.20; mean = 11.8 Hz, during pinch). Neurones in (C, D) were recorded in the same 6-OHDA-lesioned animal. Calibration bars apply to all left hand panels.

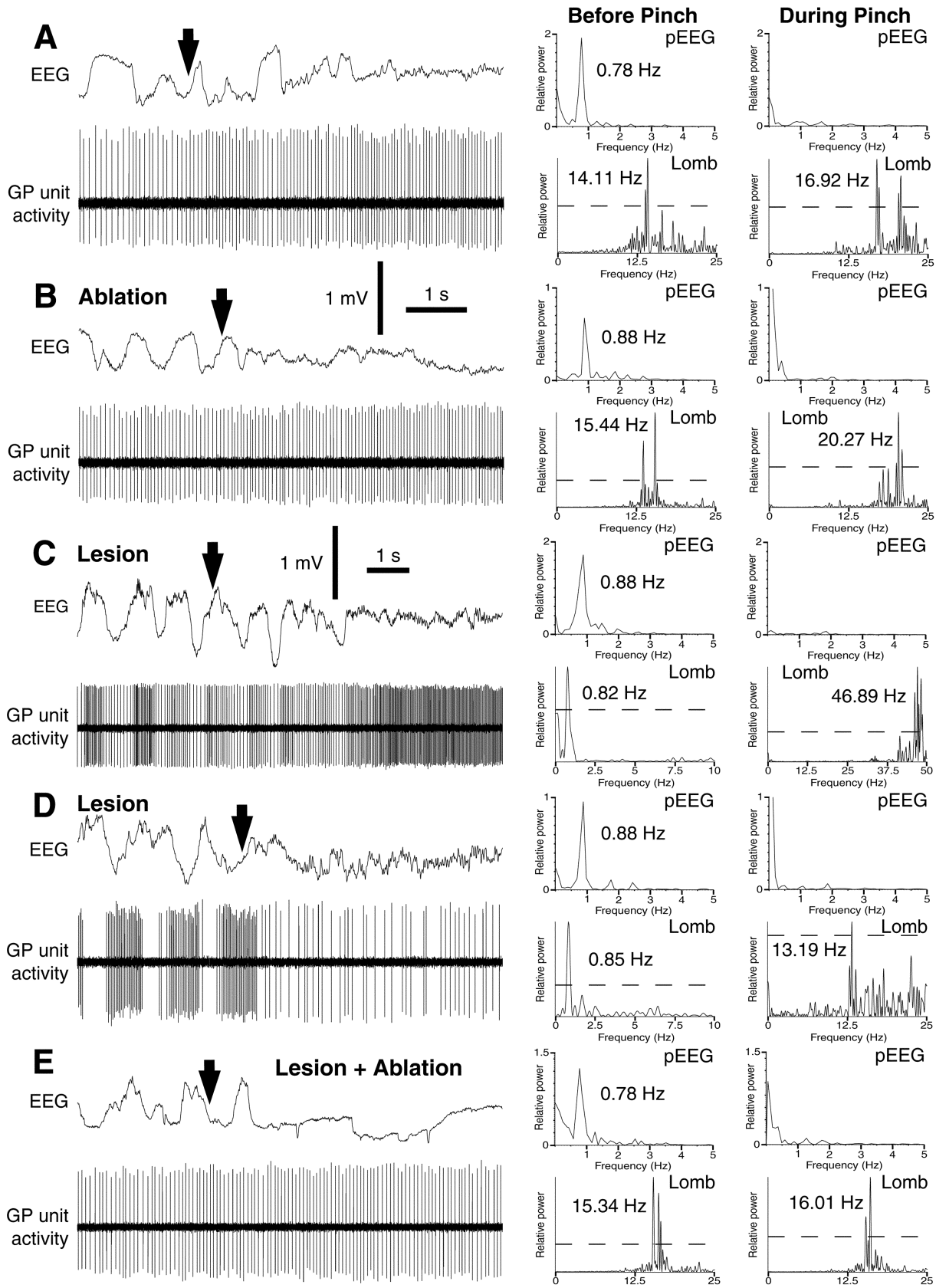
Before Pinch
During Pinch
A
EEG
GP unit activity
B Ablation
1 mV
1 s
C Lesion
D Lesion
E Lesion + Ablation
pEEG
Lomb
0.78 Hz
14.11 Hz
16.92 Hz
0.88 Hz
15.44 Hz
20.27 Hz
0.82 Hz
46.89 Hz
0.85 Hz
13.19 Hz
15.34 Hz
16.01 Hz
Relative power
Frequency (Hz)

Fig. 7.

Table 3. Responses of STN and GP neurones to global activation

		Control		6-OHDA-lesioned	
		Intact cortex	Ablated cortex	Intact cortex	Ablated cortex
STN	Number of neurones tested	17	7	16	9
	Percent of neurones that increased firing	100	100	100	100
	Percent increase in firing	145.5 ± 32.0	131.7 ± 28.7	228.6 ± 100.0	150.6 ± 62.0
GP	Number of neurones tested	16	9	23	12
	Percent of neurones that increased firing	100	100	39	100
	Percent increase in firing	142.0 ± 19.1	120.7 ± 11.2	134.3 ± 22.6	121.2 ± 19.8
	Percent of neurones that decreased firing	0	0	61	0
	Percent decrease in firing	–	–	58.3 ± 23.5	–

Data expressed as mean ± S.D.

6-OHDA-lesioned animals exhibited decreased rates of activity during coincident cortical activation [Fig. 7D, Table 3; 58.3 ± 23.5% of spontaneous firing rates, $n = 14$ (3 of 14 fired predominantly during the active component before pinch), $P = 0.001$]. The firing rates of the remaining GP neurones increased during activation [Fig. 7C; 134.3 ± 22.6%, $n = 9$ (two of nine fired predominantly during the active component before pinch), $P = 0.008$]. The mean firing rate (prior to hindpaw pinch) and the spatial distribution of GP neurones that decreased or increased their activity during global activation were similar (data not shown). LFO activity in the GP in 6-OHDA-lesioned animals resumed only when SWA reappeared in the EEG (data not shown).

Subsequent to ipsilateral cortical ablation, sensory stimulation was accompanied by changes in the rate and pattern of firing of GP neurones (Fig. 7B, E). Indeed, GP neurones adopted uniformly a tonic, regular firing pattern with an increased mean rate in control and 6-OHDA-lesioned animals (Fig. 7B, E, respectively; Table 3; firing rates of GP neurones in control animals increased to 120.7 ± 11.2% of spontaneous firing rates, $n = 9$, $P = 0.001$; firing rates of GP neurones in dopamine-depleted animals increased to 121.2 ± 19.8%, $n = 12$, $P = 0.005$). Alterations in firing pattern during global activation were minor and were evident as small changes in CVs (Fig. 7B, E). Taken together, these observations indicate that global activation results in a shift in the activity of the STN–GP network away from LFO firing patterns and that subcortical structures may play a role in this effect. Furthermore, these data suggest that the response of the STN–GP network to sensory stimulation is altered dramatically by the depletion of dopamine and that corticofugal pathways are critical to these changes.

DISCUSSION

The more intense LFO activity in the STN–GP network following dopamine depletion is driven predominantly by the cortex

The EEGs of rats anaesthetised with urethane were dominated by a low-frequency oscillation (~1 Hz) that was similar in form to that described previously in naturally sleeping or anaesthetised rats, cats and humans (Steriade et al., 1993c, 1996; Achermann and Borbély, 1997; Amzica and Steriade, 1998; Steriade and Amzica, 1998; Magill et al., 2000; Urbain et al., 2000). The slow oscillation is generated by synchronous, rhythmic depolarising (active component) and hyperpolarising (inactive component) transitions in the membrane potential of principal cortical neurones (Steriade et al., 1993c;

Fig. 7. Cortical activation increases the firing rates of GP neurones in control rats but may increase or decrease the firing rates of GP neurones in 6-OHDA-lesioned animals. (A) Regular firing GP neurone recorded in a control animal (CV = 0.21; mean = 14.2 Hz, before pinch). Typical response to cortical activation (evoked by a 7 s hindpaw pinch; starts at arrow). The loss of SWA resulted in slightly more irregular firing and an increase in the mean firing rate (CV = 0.24; mean = 18.9 Hz, during pinch). (B) Regular firing GP neurone recorded in a control animal after cortical ablation (CV = 0.17; mean = 14.4 Hz, before pinch). Disruption of contralateral SWA by pinching the hindpaw (arrow) increased the mean firing rate of the GP neurone (CV = 0.19; mean = 20.2 Hz, during pinch). (C) LFO GP neurone recorded in a 6-OHDA-lesioned animal (CV = 0.60, mean = 23.1 Hz, before pinch). Abolition of cortical SWA by sensory stimulation (starts at arrow) produced an alteration in the firing pattern, from LFO firing to regular firing, and increased the mean firing rate of the GP neurone (CV = 0.12; mean = 43.6 Hz, during pinch). (D) LFO GP neurone recorded in a 6-OHDA-lesioned animal (CV = 0.96, mean = 36.5 Hz, before pinch). Obliteration of cortical SWA by sensory stimulation (arrow) produced an alteration in the firing pattern, from LFO firing to regular firing, and decreased the mean firing rate of the GP neurone (CV = 0.55; mean = 10.9 Hz, during pinch). Decreased activity of GP neurones in response to global activation was only observed in 6-OHDA-lesioned animals. LFO unit activity in (C, D) did not resume until robust SWA reappeared in the EEG (data not shown). (E) Regular firing GP neurone (CV = 0.17; mean = 15.5 Hz, before pinch) recorded in a 6-OHDA-lesioned animal after cortical ablation. Activation of contralateral cortex (arrow) produced a modest increase in the mean firing rate of the GP neurone (CV = 0.18; mean = 16.4 Hz, during pinch). All GP neurones recorded after cortical ablation increased their mean firing rates in response to the hindpaw pinch. Neurones in (A, B) were recorded in the same control animal. Neurones in (C, D) were recorded in the same 6-OHDA-lesioned animal. Calibration bars in (B) apply to (A, D, E).

Cowan and Wilson, 1994; Amzica and Steriade, 1995; Contreras and Steriade, 1995; Destexhe et al., 1999). This activity leads to synchronous discharges in corticofugal pathways, which in turn, may entrain the basal ganglia, thalamus and other subcortical structures to the slow oscillation (Steriade et al., 1993b; Stern et al., 1997; Magill et al., 2000). Indeed, we found that activity in STN neurones was correlated tightly with coincident SWA in both control and 6-OHDA-lesioned animals, and that the removal of the ipsilateral cortex largely abolished LFO activity in STN neurones. The profile of SWA and the frequency of coincident oscillatory activity in STN neurones in 6-OHDA-lesioned animals were similar to those observed in control animals. However, the intensity of LFO discharge in the STN was greater in 6-OHDA-lesioned animals. This effect was largely abolished by cortical ablation, implying that the impact of cortical SWA on the STN is greater following dopamine depletion. The removal of cortical synaptic input by ablation in control and 6-OHDA-lesioned animals typically resulted in slower, tonic firing of STN neurones, which was similar to the discharge pattern of STN neurones in deafferented, brain slice preparations (Nakanishi et al., 1987; Beurrier et al., 1999; Bevan and Wilson, 1999). Therefore, the cortex appears to act as a potent driving force of STN neuronal activity in both control and dopamine-depleted animals. The changes in activity that followed ablation were not due to shifts in states of global activation because SWA persisted in the contralateral cortex.

In confirmation of previous observations made during urethane anaesthesia (Magill et al., 2000) and in contrast to the STN, the GP was not entrained by coincident cortical SWA in control animals. Furthermore, cortical ablation in control animals had no effect on the rate or pattern of firing of GP neurones suggesting that monosynaptic and polysynaptic pathways from the cortex to the GP (Naito and Kita, 1994; for review, see Smith et al., 1998) have minimal impact on neuronal activity (Magill et al., 2000). This study therefore suggests that SWA in neurones of the corticosubthalamic pathway, rather than activity in the indirect pathway, underlies oscillatory activity in the control STN because removal of large areas of cortex had little effect on the activity of GP neurones. Taken together, our data indicate that in control animals, the STN–GP network does not support emergent LFO activity in isolation from the cortex.

In marked contrast to observations in control animals, GP neurones in 6-OHDA-lesioned animals displayed LFO firing patterns that matched the frequency of coincident SWA. However, the firing rate was not significantly different to that observed in control animals. The oscillatory firing patterns of GP neurones were likely to have been generated by more intense activity in subthalamopallidal projections because ablation of the STN in animal models of PD has been shown to regularise activity in GP and basal ganglia output nuclei (Wichmann et al., 1994b; Burbaud et al., 1995; Murer et al., 1997; Ni et al., 2000). In support of this, destruction of the cortex, which results in the abolition of oscillatory activity in the STN, led to more regular activity in the GP.

The increased rate of STN activity following 6-OHDA-lesions, or the decreased rate of STN activity following cortical ablation, were not associated with an alteration in the rate of firing of GP neurones. The poor correlations in the relative rates of activity in the STN and GP observed in this part of the study are not in keeping with the widely held direct–indirect pathway model (Albin et al., 1989; DeLong, 1990).

These findings indicate that the majority of the STN–GP network in this preparation does not support emergent oscillatory activity in isolation from the cerebral cortex. It should be stressed however, that a subpopulation of neurones in 6-OHDA-lesioned animals (20% in STN, 15% in GP) continued to display LFO activity following ipsilateral cortical ablation. It is possible that: (1) these neurones were driven by remaining parts of the cortex (Canteras et al., 1990); (2) the STN–GP network does in fact support oscillatory activity, but this activity is expressed in a minority of neurones (Plenz and Kitai, 1999); or (3) oscillatory activity was driven by intrinsic membrane properties (Nambu and Llinás, 1994; Beurrier et al., 1999).

Dopamine has multiple pre- and post-synaptic actions in each nucleus of the basal ganglia (see reviews by Greengard et al., 1999; Nicola et al., 2000; Smith and Kieval, 2000). We cannot therefore exclude the possibility that, following the loss of dopaminergic tone, pathological STN–GP network activity reverberated throughout the cortical-basal ganglia-thalamocortical loop and led to abnormal input from other afferents, which further amplified LFO activity. It is also possible that the 6-OHDA-induced degeneration of VTA neurones may have had an adverse effect on cortical activity, although we observed no differences in cortical SWA in 6-OHDA-lesioned and control animals. Furthermore, we could find no clear correlation between the extent of VTA lesion and activity patterns in the STN–GP network.

The response of the STN–GP network to cortical activation is altered by dopamine depletion and is not associated with LFO activity

Sensory stimulation by hindpaw pinch was associated with the obliteration of SWA and the appearance of smaller-amplitude, higher-frequency waves in the EEG. In control animals, this cortical activation was associated with increases in the mean firing rates of all neurones that were tested in the STN and GP. Low-frequency oscillatory activity in STN neurones was abolished during cortical activation, whereas the firing patterns of GP neurones were largely unaltered, thus confirming and extending previous observations (Magill et al., 2000). The effects of sensory stimulation on the EEG were similar to those reported previously (Détári and Vanderwolf, 1987; Nuñez, 1996; Magill et al., 2000) and were similar to those elicited by stimulation of the midbrain reticular activating system (Moruzzi and Magoun, 1949; Steriade et al., 1993a, 1996), which is known to depolarise cortical

neurones, resulting in an increase in corticofugal activity and a reduction in global synchrony (Steriade et al., 1993a, 1996). Thus, the increased activity observed in the STN–GP network is probably driven, at least in part, by the cortex. Excitatory subcortical afferents (e.g. intralaminar thalamic nuclei, pedunculopontine nucleus and dorsal raphe nucleus) probably also contributed to responses since increases in network activity were still observed following cortical ablation (Peschanski et al., 1981; Rouzaire-Dubois and Scarnati, 1987; Canteras et al., 1990; Garcia-Rill, 1991; Bevan and Bolam, 1995; Mouroux et al., 1995, see review by Smith et al., 1998).

Sensory stimulation by hindpaw pinch in 6-OHDA-lesioned animals also led to cortical activation, which was similar in profile to that observed in control animals and abolished LFO activity in the STN–GP network. However, cortical activation in 6-OHDA-lesioned animals increased the activity of STN neurones to a greater degree than in control animals. In clear distinction to GP responses in control animals, both inhibition and facilitation of the activity of GP neurones was observed. Cortical ablation in 6-OHDA-lesioned animals led to a loss of inhibitory GP responses to sensory stimulation. The inhibitory responses in the GP could not have arisen from decreased activity in the STN because all STN neurones significantly increased their firing rates. Since activity of GP neurones is largely governed by inputs from the STN and the striatum (Ryan and Clark, 1991; Kita and Kitai, 1991; Kita, 1992; Yoshida et al., 1993; Smith et al., 1998), as well as intrinsic membrane properties (Nambu and Llinás, 1994; Cooper and Stanford, 2000), and all STN neurones were excited during global activation in 6-OHDA-lesioned rats with intact cortices, the inhibition of GP activity was probably the result of cortical activation of the striatum and, hence, the indirect pathway. Indeed, the direct–indirect pathway model of basal ganglia pathophysiology (Albin et al., 1989; DeLong, 1990) predicts that the indirect pathway is overactive in the parkinsonian brain. However, the possibility that other inputs to GP neurones (reviewed by Smith et al., 1998) are important cannot be ruled out. Furthermore, the increases in activity in the GP that were also observed during cortical activation in 6-OHDA-lesioned animals suggest that the relationship between the STN and GP cannot be accounted for simply in terms of firing rate and that the situation is much more complex than predicted by the model.

Implications for information processing in the STN–GP network in the dopamine-depleted brain

The principal findings of this study are that oscillatory cortical activity is expressed more powerfully by the STN–GP network in the dopamine-depleted brain and that the manner in which cortical information is processed by the network is altered profoundly by the chronic depletion of dopamine. Oscillatory activity in the network is largely abolished by removal of rhythmic cortical input. The increased sensitivity of the dopamine-depleted basal ganglia to rhythmic cortical activity implies that resting LFO activity in the basal ganglia of PD patients (Rodriguez et al., 1998; Magariños-Ascone et al., 2000; Magnin et al., 2000) could be due to abnormal sensitivity of the diseased basal ganglia to low-frequency cortical rhythms associated with quiet wakefulness (Alberts et al., 1969; Elble and Koller, 1990; Volkmann et al., 1996; Llinás et al., 1999; Hellwig et al., 2000). However, it should also be noted that a component of the STN–GP network continues to oscillate independently of the cortex in the 6-OHDA-lesioned hemisphere, implying that intrinsic properties of this network may also pattern oscillatory activity in PD (Nambu and Llinás, 1994; Beurrier et al., 1999; Plenz and Kitai, 1999). Since a small proportion of neurones may not require rhythmic corticosubthalamic input to generate LFO activity following dopamine depletion, it is possible that the cortical-basal ganglia-thalamocortical loop instead acts to relay and amplify abnormal oscillatory activity generated by a subpopulation of neurones within the STN–GP network. As LFO activity in the brain is associated with long-term changes in synaptic efficacy, abnormal, intense oscillatory activity in the dopamine-depleted brain may be consolidated during sleep and/or wakefulness, and further worsen the symptoms of PD (Kavanau, 1997; Charpier et al., 1999; Steriade, 1999).

The augmentation of the indirect pathway during global activation indicates that inputs from the activated cortex are processed differently by the dopamine-depleted basal ganglia. Indeed, incorrect integration of cortical information has been proposed to underlie, in part, the symptoms of PD (Filion et al., 1988; DeLong, 1990; Bergman et al., 1994; Rothblat and Schneider, 1995; Calabresi et al., 1996; Boraud et al., 2000).

Taken together, the results of this and other studies demonstrate that both the rate and pattern of activity of basal ganglia neurones are altered profoundly by chronic dopamine-depletion. Furthermore, the relative contribution of rate and pattern to aberrant information coding is related to the state of activation of the cerebral cortex.

Acknowledgements—This work was supported by the Medical Research Council UK and the European Community (BIOMED 2 project Grant BMH4-CT-97-2215). P.J.M. was in receipt of a Medical Research Council studentship. We gratefully acknowledge Dr. Y. Kaneoke for the provision of the oscillation detection algorithm and Dr. E.A. Stern for the correlation analysis routines. We thank Caroline Francis for expert technical assistance and Paul Jays for image processing.

REFERENCES

Abeles, M., 1982. Quantification, smoothing, and confidence limits for single-units' histograms. J. Neurosci. Methods 5, 317–325.
Achermann, P., Borbély, A.A., 1997. Low-frequency (< 1 Hz) oscillations in the human sleep electroencephalogram. Neuroscience 81, 213–222.
Alberts, W.W., Wright, E.W., Feinstein, B., 1969. Cortical potentials and parkinsonian tremor. Nature 221, 670–672.
Albin, R.L., Young, A.B., Penney, J.B., 1989. The functional anatomy of basal ganglia disorders. Trends Neurosci. 12, 366–375.

Aldridge, J.W., Gilman, S., 1991. The temporal structure of spike trains in the primate basal ganglia: afferent regulation of bursting demonstrated with precentral cerebral cortical ablation. Brain Res. 543, 123–138.
Alexander, G.E., Crutcher, M.D., 1990. Functional architecture of basal ganglia circuits: neural substrates of parallel processing. Trends Neurosci. 13, 266–271.
Amzica, F., Steriade, M., 1995. Short- and long-range neuronal synchronization of the slow (<1 Hz) cortical oscillation. J. Neurophysiol. 73, 20–37.
Amzica, F., Steriade, M., 1998. Cellular substrate and laminar profile of sleep K-complex. Neuroscience 82, 671–686.
Anderson, M.E., Turner, R.S., 1991. A quantitative analysis of pallidal discharge during targeted reaching movement in the monkey. Exp. Brain Res. 86, 623–632.
Benazzouz, A., Gross, C., Féger, J., Boraud, T., Bioulac, B., 1993. Reversal of rigidity and improvement in motor performance by subthalamic high-frequency stimulation in MPTP-treated monkeys. Eur. J. Neurosci. 5, 382–389.
Bergman, H., Wichmann, T., Karmon, B., DeLong, M.R., 1994. The primate subthalamic nucleus. II. Neuronal activity in the MPTP model of Parkinsonism. J. Neurophysiol. 72, 507–520.
Bergman, H., Feingold, A., Nini, A., Raz, A., Slovin, H., Abeles, M., Vaadia, E., 1998. Physiological aspects of information processing in the basal ganglia of normal and parkinsonian primates. Trends Neurosci. 21, 32–38.
Beurrier, C., Congar, P., Bioulac, B., Hammond, C., 1999. Subthalamic nucleus neurones switch from single-spike activity to burst-firing mode. J. Neurosci. 19, 599–609.
Bevan, M.D., Bolam, J.P., 1995. Cholinergic, GABAergic, and glutamate-enriched inputs from the mesopontine tegmentum to the subthalamic nucleus in the rat. J. Neurosci. 15, 7105–7120.
Bevan, M.D., Wilson, C.J., 1999. Mechanism underlying spontaneous oscillation and rhythmic firing in rat subthalamic neurones. J. Neurosci. 19, 7617–7628.
Bevan, M.D., Francis, C.F., Bolam, J.P., 1995. The glutamate-enriched cortical and thalamic input to neurones in the subthalamic nucleus of the rat. J. Comp. Neurol. 361, 491–511.
Bevan, M.D., Booth, P.A.C., Eaton, S.A., Bolam, J.P., 1998. Selective innervation of neostriatal interneurones by a subclass of neuron in the globus pallidus of the rat. J. Neurosci. 18, 9438–9452.
Bolam, J.P. (Ed.), 1992. Experimental Neuroanatomy. Oxford University Press, Oxford.
Boraud, T., Bezard, E., Guehl, D., Bioulac, B., Gross, C., 1998. Effects of L-DOPA on neuronal activity of the globus pallidus externalis (GPe) and globus pallidus internalis (GPi) in the MPTP-treated monkey. Brain Res. 787, 157–160.
Boraud, T., Bezard, E., Bioulac, B., Gross, C.E., 2000. Ratio of inhibited-to-activated pallidal neurones decreases dramatically during passive limb movement in the MPTP-treated monkey. J. Neurophysiol. 83, 1760–1763.
Burbaud, P., Gross, C., Benazzouz, A., Coussemacq, M., Bioulac, B., 1995. Reduction of apomorphine-induced rotational behaviour by subthalamic lesion in 6-OHDA lesioned rats is associated with a normalization of firing rate and discharge pattern in pars reticulata neurones. Exp. Brain Res. 105, 48–58.
Calabresi, P., Pisani, A., Mercuri, N.B., Bernardi, G., 1996. The corticostriatal projection: from synaptic plasticity to dysfunctions of the basal ganglia. Trends Neurosci. 19, 19–24.
Canteras, N.S., Shammah-Lagnado, S.J., Silva, B.A., Ricardo, J.A., 1990. Afferent connections of the subthalamic nucleus; a combined retrograde and anterograde horseradish peroxidase study in the rat. Brain Res. 513, 43–59.
Charpier, S., Mahon, S., Deniau, J.M., 1999. *In vivo* induction of long-term potentiation by low-frequency stimulation of the cerebral cortex. Neuroscience 91, 1209–1222.
Chesselet, M.F., Delfs, J.M., 1995. Basal ganglia and movement disorders. Trends Neurosci. 19, 417–422.
Contreras, D., Steriade, M., 1995. Cellular basis of EEG slow rhythms: a study of dynamic corticothalamic relationships. J. Neurosci. 15, 604–622.
Cooper, A.J., Stanford, I.M., 2000. Electrophysiological and morphological characteristics of three subtypes of rat globus pallidus neurone *in vitro*. J. Physiol. 527, 291–304.
Cowan, R.L., Wilson, C.J., 1994. Spontaneous firing patterns and axonal projections of single corticostriatal neurones in the rat medial agranular cortex. J. Neurophysiol. 71, 17–32.
DeLong, M.R., 1990. Primate models of movement disorders of basal ganglia origin. Trends Neurosci. 13, 281–285.
DeLong, M.R., Crutcher, M.D., Georgopoulos, A.P., 1985. Primate globus pallidus and subthalamic nucleus: functional organization. J. Neurophysiol. 53, 530–543.
Destexhe, A., Contreras, D., Steriade, M., 1999. Spatiotemporal analysis of local field potentials and unit discharges in cat cerebral cortex during natural wake and sleep states. J. Neurosci. 19, 4595–4608.
Détári, L., Vanderwolf, C.H., 1987. Activity of identified cortically projecting and other basal forebrain neurones during large slow-waves and cortical activation in anaesthetized rats. Brain Res. 437, 1–8.
Elble, R.J., Koller, W.C., 1990. Parkinsonian tremor. In: Tremor. Johns Hopkins University Press, Baltimore, MD, pp. 118–133.
Filion, M., 1979. Effects of interruption of the nigrostriatal pathway and of dopaminergic agents on the spontaneous activity of globus pallidus neurones in the awake monkey. Brain Res. 178, 425–441.
Filion, M., Tremblay, L., 1991. Abnormal spontaneous activity of globus pallidus neurones in monkeys with MPTP-induced Parkinsonism. Brain Res. 547, 142–151.
Filion, M., Tremblay, L., Bédard, P.J., 1988. Abnormal influences of passive limb movement on the activity of globus pallidus neurones in parkinsonian monkeys. Brain Res. 444, 165–176.
Fujimoto, K., Kita, H., 1993. Response characteristics of subthalamic neurones to the stimulation of the sensorimotor cortex in the rat. Brain Res. 609, 185–192.
Garcia-Rill, E., 1991. The pedunculopontine nucleus. Prog. Neurobiol. 36, 363–389.
Georgopoulos, A.P., DeLong, M.R., Crutcher, M.D., 1983. Relations between parameters of step-tracking movements and single cell discharge in the globus pallidus and subthalamic nucleus of the behaving monkey. J. Neurosci. 3, 1586–1598.
Gerfen, C.R., Wilson, C.J., 1996. The basal ganglia. In: Swanson, L.W., Björklund A., Hökfelt T. (Eds.), Handbook of Chemical Neuroanatomy: Integrated Systems of the CNS III, Vol. 12. Elsevier, London, pp. 371–468.
Graybiel, A.M., 1995. Building action repertoires: memory and learning functions of the basal ganglia. Curr. Opin. Neurobiol. 5, 733–741.
Greengard, P., Allen, P.B., Nairn, A.C., 1999. Beyond the dopamine receptor: the DARPP-32/protein phosphatase-1 cascade. Neuron 23, 435–447.
Hassani, O.K., Mouroux, M., Féger, J., 1996. Increased subthalamic neuronal activity after nigral dopaminergic lesion independent of disinhibition via the globus pallidus. Neuroscience 72, 105–115.
Hellwig, B., Häußler, S., Lauk, M., Guschlbauer, B., Köster, B., Krsietva-Feige, R., Timmer, J., Lücking, C.H., 2000. Tremor-correlated cortical activity detected by electroencephalography. Clin. Neurophysiol. 111, 806–809.

Hollerman, J.R., Grace, A.A., 1992. Subthalamic nucleus cell firing in the 6-OHDA-treated rat: basal activity and response to haloperidol. Brain Res. 590, 291–299.
Horikawa, K., Armstrong, W.E., 1991. A biocytin-containing compound N-(2-aminoethyl)biotinimide for intracellular labeling and neuronal tracing studies: comparison with biocytin. J. Neurosci. Methods 37, 141–150.
Hudson, J.L., van Horne, C.G., Strömberg, I., Brock, S., Clayton, J., Masserano, J., Hoffer, B.J., Gerhardt, G.A., 1993. Correlation of apomorphine- and amphetamine-induced turning with nigrostriatal dopamine content in unilateral 6-hydroxydopamine lesioned rats. Brain Res. 626, 167–174.
Johnson, D.H., 1996. Point process models of single-neuron discharges. J. Comput. Neurosci. 3, 275–299.
Kaneoke, Y., Vitek, J.L., 1996. Burst and oscillation as disparate neuronal properties. J. Neurosci. Methods 68, 221–223.
Kavanau, J.L., 1997. Memory, sleep and the evolution of mechanisms of synaptic efficacy maintenance. Neuroscience 79, 7–44.
Kita, H., 1992. Responses of globus pallidus neurones to cortical stimulation: intracellular study in the rat. Brain Res. 589, 84–90.
Kita, H., Kitai, S.T., 1991. Intracellular study of rat globus pallidus neurones: membrane properties and responses to neostriatal, subthalamic and nigral stimulation. Brain Res. 564, 296–305.
Kitai, S.T., Deniau, J.M., 1981. Cortical inputs to the subthalamus: intracellular analysis. Brain Res. 214, 411–415.
Krack, P., Benazzouz, A., Pollak, P., Limousin, P., Piallat, B., Hoffmann, D., Xie, J., Benabid, A.L., 1998. Treatment of tremor in Parkinson's disease by subthalamic nucleus stimulation. Mov. Disord. 13, 907–914.
Kreiss, D.S., Mastropietro, C.W., Rawji, S.S., Walters, J.R., 1997. The responses of subthalamic nucleus neurones to dopamine receptor stimulation in a rodent model of Parkinson's Disease. J. Neurosci. 17, 6807–6819.
Levy, R., Hazrati, L.N., Herrero, M.T., Vila, M., Hassani, O.K., Mouroux, M., Ruberg, M., Asensi, H., Agid, Y., Féger, J., Obeso, J.A., Parent, A., Hirsch, E.C., 1997. Re-evaluation of the functional anatomy of the basal ganglia in normal and parkinsonian states. Neuroscience 76, 335–343.
Limousin, P., Pollak, P., Benazzouz, A., Hoffmann, D., Le Bas, J.F., Broussolle, E., Perret, J.E., Benabid, A.L., 1995. Effect on parkinsonian signs and symptoms of bilateral subthalamic nucleus stimulation. Lancet 345, 91–95.
Llinás, R.R., Ribary, U., Jeanmonod, D., Kronberg, E., Mitra, P.P., 1999. Thalamocortical dysrhythmia: A neurological and neuropsychiatric syndrome characterized by magnetoencephalography. Proc. Natl. Acad. Sci. USA 96, 15222–15227.
Magariños-Ascone, C.M., Figueiras-Mendez, R., Riva-Meana, C., Córdoba-Fernández, A., 2000. Subthalamic neuron activity related to tremor and movement in Parkinson's disease. Eur. J. Neurosci. 12, 2597–2607.
Magill, P.J., Bolam, J.P., Bevan, M.D., 2000. Relationship of activity in the subthalamic nucleus-globus pallidus network to cortical electroencephalogram. J. Neurosci. 20, 820–833.
Magnin, M., Morel, A., Jeanmonod, D., 2000. Single-unit analysis of the pallidum, thalamus and subthalamic nucleus in parkinsonian patients. Neuroscience 96, 549–564.
Maurice, N., Deniau, J.M., Glowinski, J., Thierry, A.M., 1998. Relationships between the prefrontal cortex and the basal ganglia in the rat: physiology of the corticosubthalamic circuits. J. Neurosci. 18, 9539–9546.
McCormick, D.A., Bal, T., 1997. Sleep and arousal: thalamocortical mechanisms. Annu. Rev. Neurosci. 20, 185–215.
Moruzzi, G., Magoun, H.W., 1949. Brain stem reticular formation and activation of the EEG. Electroencephalogr. Clin. Neurophysiol. 1, 455–473.
Mouroux, M., Hassani, O.K., Féger, J., 1995. Electrophysiological study of the excitatory parafascicular projection to the subthalamic nucleus and evidence for ipsi- and contralateral controls. Neuroscience 67, 399–407.
Murer, M.G., Riquelme, L.A., Tseng, K.Y., Pazo, J.H., 1997. Substantia nigra pars reticulata single unit activity in normal and 6-OHDA-lesioned rats: effects of intrastriatal apomorphine and subthalamic lesions. Synapse 27, 278–293.
Naito, A., Kita, H., 1994. The cortico-pallidal projection in the rat: an anterograde tracing study with biotinylated dextran amine. Brain Res. 653, 251–257.
Nakanishi, H., Kita, H., Kitai, S.T., 1987. Electrical membrane properties of rat subthalamic neurones in an *in vitro* slice preparation. Brain Res. 437, 35–44.
Nambu, A., Llinás, R., 1994. Electrophysiology of globus pallidus neurones *in vitro*. J. Neurophysiol. 72, 1127–1139.
Nambu, A., Yoshida, S.I., Jinnai, K., 1990. Discharge patterns of pallidal neurones with input from various cortical areas during movement in the monkey. Brain Res. 519, 183–191.
Ni, Z., Bouali-Benazzouz, R., Gao, D., Benabid, A.L., Benazzouz, A., 2000. Changes in the firing pattern of globus pallidus neurones after the degeneration of nigrostriatal pathway are mediated by the subthalamic nucleus in the rat. Eur. J. Neurosci. 12, 4338–4344.
Nicola, S.M., Surmeier, D.J., Malenka, R.C., 2000. Dopaminergic modulation of neuronal excitability in the striatum and nucleus accumbens. Annu. Rev. Neurosci. 23, 185–215.
Nini, A., Feingold, A., Slovin, H., Bergman, H., 1995. Neurones in the globus pallidus do not show correlated activity in the normal monkey, but phase-locked oscillations appear in the MPTP model of Parkinsonism. J. Neurophysiol. 74, 1800–1805.
Nuñez, A., 1996. Unit activity of rat basal forebrain neurones: relationship to cortical activity. Neuroscience 72, 757–766.
Obeso, J.A., Rodríguez-Oroz, M.C., Rodríguez, M., Lanciego, J.L., Artieda, J., Gonzalo, N., Olanow, C.W., 2000. Pathophysiology of the basal ganglia in Parkinson's disease. Trends Neurosci. 23 (Suppl. 10), S8–S19.
Pan, H.S., Walters, J.R., 1988. Unilateral lesion of the nigrostriatal pathway decreases the firing rate and alters the firing pattern of globus pallidus neurones in the rat. Synapse 2, 650–656.
Paxinos, G., Watson, C., 1986. The rat brain in stereotaxic coordinates, 2nd edn. Academic Press, Sydney.
Perkel, D.H., Gerstein, G.L., Moore, G.P., 1967. Neuronal spike trains and stochastic point processes II. simultaneous spike trains. Biophys. J. 7, 419–440.
Peschanski, M., Guilbaud, G., Gautron, M., 1981. Posterior intralaminar region in rat: neuronal responses to noxious and non-noxious cutaneous stimuli. Exp. Neurol. 72, 226–238.
Pinault, D., 1996. A novel single-cell staining procedure performed *in vivo* under electrophysiological control: morpho-functional features of juxtacellularly labeled thalamic cells and other central neurones with biocytin or Neurobiotin. J. Neurosci. Methods 65, 113–136.
Plenz, D., Kitai, S.T., 1999. A basal ganglia pacemaker formed by the subthalamic nucleus and external globus pallidus. Nature 400, 677–682.
Raz, A., Vaadia, E., Bergman, H., 2000. Firing patterns and correlations of spontaneous discharge of pallidal neurones in the normal and the tremulous 1-methyl-4-phenyl-1,2,3,6-tetrahydropyridine vervet model of parkinsonism. J. Neurosci. 20, 8559–8571.
Rodriguez, M.C., Guridi, O.J., Alvarez, L., Mewes, K., Macias, R., Vitek, J., DeLong, M.R., Obeso, J.A., 1998. The subthalamic nucleus and tremor in Parkinson's disease. Mov. Disord. 13 (Suppl. 3), 111–118.
Rothblat, D.S., Schneider, J.S., 1995. Alterations in pallidal neuronal responses to peripheral sensory and striatal stimulation in symptomatic and recovered parkinsonian cats. Brain Res. 705, 1–14.
Rouzaire-Dubois, B., Scarnati, E., 1985. Bilateral corticosubthalamic nucleus projections: electrophysiological study in rats with chronic cerebral lesions. Neuroscience 15, 69–79.

Rouzaire-Dubois, B., Scarnati, E., 1987. Pharmacological study of the cortical-induced excitation of subthalamic e in the rat: evidence for amino acids as putative neurotransmitters. Neuroscience 21, 429–440.
Ryan, L.J., Clark, K.B., 1991. The role of the subthalamic nucleus in the response of globus pallidus neurones to stimulation of the prelimbic and agranular frontal cortices in rats. Exp. Brain Res. 86, 641–651.
Ryan, L.J., Clark, K.B., 1992. Alteration of neuronal responses in the subthalamic nucleus following globus pallidus and neostriatal lesions in rats. Brain Res. Bull. 29, 319–327.
Ryan, L.J., Sanders, D.J., Clark, K.B., 1992. Auto- and cross-correlation analysis of subthalamic nucleus neuronal activity in neostriatal- and globus pallidal-lesioned rats. Brain Res. 583, 253–261.
Schultz, W., Tremblay, L., Hollerman, J.R., 1998. Reward prediction in primate basal ganglia and frontal cortex. Neuropharmacology 37, 421–429.
Schwarting, R.K.W., Huston, J.P., 1996a. Unilateral 6-hydroxydopamine lesions of meso-striatal dopamine neurones and their physiological sequelae. Prog. Neurobiol. 49, 215–266.
Schwarting, R.K.W., Huston, J.P., 1996b. The unilateral 6-hydroxydopamine lesion model in behavioral brain research. Analysis of functional deficits, recovery and treatments. Prog. Neurobiol. 50, 275–331.
Shink, E., Bevan, M.D., Bolam, J.P., Smith, Y., 1996. The subthalamic nucleus and the external pallidum: two tightly interconnected structures that control the output of the basal ganglia in the monkey. Neuroscience 73, 335–357.
Smith, Y., Kieval, J.Z., 2000. Anatomy of the dopamine system in the basal ganglia. Trends Neurosci. 23 (Suppl. 10), S28–S33.
Smith, Y., Bevan, M.D., Shink, E., Bolam, J.P., 1998. Microcircuitry of the direct and indirect pathways of the basal ganglia. Neuroscience 86, 353–387.
Steriade, M., 1999. Coherent oscillations and short-term plasticity in corticothalamic networks. Trends Neurosci. 22, 337–345.
Steriade, M., Amzica, F., 1998. Coalescence of sleep rhythms and their chronology in corticothalamic networks. Sleep Res. Online 1, 1–10.
Steriade, M., Amzica, F., Nuñez, A., 1993a. Cholinergic and noradrenergic modulation of the slow ($\approx$0.3 Hz) oscillation in neocortical cells. J. Neurophysiol. 70, 1385–1400.
Steriade, M., Contreras, D., Curró Dossi, R., Nuñez, A., 1993b. The slow ($<$1 Hz) oscillation in reticular thalamic and thalamocortical neurones: scenario of sleep rhythm generation in interacting thalamic and neocortical networks. J. Neurosci. 13, 3284–3299.
Steriade, M., Nuñez, A., Amzica, F., 1993c. A novel slow ($<$1 Hz) oscillation of neocortical neurones *in vivo*: depolarizing and hyperpolarizing components. J. Neurosci. 13, 3252–3265.
Steriade, M., Nuñez, A., Amzica, F., 1993d. Intracellular analysis of relations between the slow ($<$1 Hz) neocortical oscillation and other sleep rhythms of the electroencephalogram. J. Neurosci. 13, 3266–3283.
Steriade, M., Contreras, D., Amzica, F., Timofeev, I., 1996. Synchronization of fast (30–40 Hz) spontaneous oscillations in intrathalamic and thalamocortical networks. J. Neurosci. 16, 2788–2808.
Stern, E.A., Kincaid, A.E., Wilson, C.J., 1997. Spontaneous subthreshold membrane potential fluctuations and action potential variability of rat corticostriatal and striatal neurones *in vivo*. J. Neurophysiol. 77, 1697–1715.
Ungerstedt, U., 1968. 6-hydroxy-dopamine induced degeneration of central monoamine neurones. Eur. J. Pharm. 5, 107–110.
Urbain, N., Gervasoni, D., Soulière, F., Lobo, L., Rentéro, N., Windels, F., Astier, B., Savasta, M., Fort, P., Renaud, B., Luppi, P.H., Chouvet, G., 2000. Unrelated course of subthalamic nucleus and globus pallidus neuronal activities across vigilance states in the rat. Eur. J. Neurosci. 12, 3361–3374.
Vila, M., Périer, C., Féger, J., Yelnik, Y., Faucheux, B., Ruberg, M., Raisman-Vozari, R., Agid, Y., Hirsch, E.C., 2000. Evolution of changes in neuronal activity in the subthalamic nucleus of rats with unilateral lesions of the substantia nigra assessed by metabolic and electrophysiological measurements. Eur. J. Neurosci. 12, 337–344.
Volkmann, J., Joliot, M., Mogilner, A., Ioannides, A.A., Lado, F., Fazzini, E., Ribary, U., Llinás, R., 1996. Central motor loop oscillations in parkinsonian resting tremor revealed by magnetoencephalography. Neurology 46, 1359–1370.
Wichmann, T., Bergman, H., DeLong, M.R., 1994a. The primate subthalamic nucleus. I. functional properties in intact animals. J. Neurophysiol. 72, 494–506.
Wichmann, T., Bergman, H., DeLong, M.R., 1994b. The primate subthalamic nucleus. III. Changes in motor behaviour and neuronal activity in the internal pallidum induced by subthalamic inactivation in the MPTP model of Parkinsonism. J. Neurophysiol. 72, 521–530.
Wichmann, T., DeLong, M.R., 1996. Functional and pathophysiological models of the basal ganglia. Curr. Opin. Neurobiol. 6, 751–758.
Yoshida, S., Nambu, A., Jinnai, K., 1993. The distribution of the globus pallidus neurones with input from various cortical areas in the monkey. Brain Res. 611, 170–174.

(*Accepted* 28 *June* 2001)